

by a Grant from the Research for the Future Program 'Molecular mechanisms on regulation of morphogenesis and metabolism leading to increased plant productivity' (No. 00L01605, K. Y.) from the Ministry of Education, Culture, Sports, Science and Technology of Japan. We are also grateful for support from the Takeda Foundation to K.Y.

## References

- Ambudkar, S.V., Dey, S., Hrycyna, C.A., Ramachandra, M., Pastan, I. and Gottesman, M.M. 1999. Biochemical, cellular, and pharmacological aspects of the multidrug transporter. *Annu. Rev. Pharmacol. Toxicol.* 39: 361–398.
- Bradley, G., Naik, M. and Ling, V. 1989. P-glycoprotein expression in multidrug-resistant human ovarian carcinoma cell lines. *Cancer Res.* 49: 2790–2796.
- Deeley, R.G. and Cole, S.P. 1997. Function, evolution and structure of multidrug resistance protein (MRP). *Semin Cancer Biol.* 8: 193–204.
- Di Virgilio, F., Fasolato, C. and Steinberg, T.H. 1988. Inhibitors of membrane transport system for organic anions block fura-2 excretion from PC12 and N2A cells. *Biochem. J.* 256: 959–963.
- Doty, S.L., Shang, T.Q., Wilson, A.M., Tangen, J., Westergreen, A.D., Newman, L.A., Strand, S.E. and Gordon, M.P. 2000. Enhanced metabolism of halogenated hydrocarbons in transgenic plants containing mammalian cytochrome P450 2E1. *Proc. Natl. Acad. Sci. USA* 97: 6287–6291.
- Higgins, C.F. 1992. ABC transporters: from microorganisms to man. *Annu. Rev. Cell Biol.* 8: 67–113.
- Hirschi, K.D., Korenkov, V.D., Wilganowski, N.L. and Wagner, G.J. 2000. Expression of arabidopsis CAX2 in tobacco. Altered metal accumulation and increased manganese tolerance. *Plant Physiol.* 124: 125–133.
- Horsh, R.B., Fry, J., Hoffman, H.L., Eicholts, D., Rogers, S.G. and Fraley, R.T. 1985. Simple and general method for transferring genes into plants. *Science* 277: 1229–1231.
- Ishikawa, T., Bao, J.J., Yamane, Y., Akimaru, K., Frindrich, K., Wright, C.D. and Kuo, M.T. 1996. Coordinated induction of MRP/GS-X pump and gamma-glutamylcysteine synthetase by heavy metals in human leukemia cells. *J. Biol. Chem.* 271: 14981–14988.
- Jedlitschky, G., Leier, I., Buchholz, U., Barnouin, K., Kurz, G. and Keppler, D. 1996. Transport of glutathione, glucuronate, and sulfate conjugates by the MRP gene-encoded conjugate export pump. *Cancer Res.* 56: 988–994.
- Liu, G., Sanchez-Fernandez, R., Li, Z.S. and Rea, P.A. 2001. Enhanced multispecificity of arabidopsis vacuolar multidrug resistance-associated protein-type ATP-binding cassette transporter, AtMRP2. *J. Biol. Chem.* 276: 8648–8656.
- Loe, D.W., Deeley, R.G. and Cole, S.P. 1996. Biology of the multidrug resistance-associated protein, MRP. *Eur. J. Cancer* 32A: 945–957.
- Lu, Y.P., Li, Z.S. and Rea, P.A. 1997. AtMRP1 gene of *Arabidopsis* encodes a glutathione S-conjugate pump: isolation and functional definition of a plant ATP-binding cassette transporter gene. *Proc. Natl. Acad. Sci. USA* 94: 8243–8248.
- Martinoia, E., Massonneau, A. and Frangne, N. 2000. Transport processes of solutes across the vacuolar membrane of higher plants. *Plant Cell Physiol.* 41: 1175–1186.
- Mitsuda, N., Takeyasu, K. and Sato, M.H. 2001. Pollen-specific regulation of vacuolar H<sup>+</sup>-PPase expression by multiple cis-acting elements. *Plant Mol. Biol.* 46: 185–192.
- Mol, J.N., van der Krol, A.R., van Tunen, A.J., van Blokland, R., de Lange, P. and Stuitje, A.R. 1990. Regulation of plant gene expression by antisense RNA. *FEBS Lett.* 268: 427–430.
- Morsomme, P., Dambly, S., Maudoux, O. and Boutry, M. 1998. Single point mutations distributed in 10 soluble and membrane regions of the *Nicotiana plumbaginifolia* plasma membrane PMA2 H<sup>+</sup>-ATPase activate the enzyme and modify the structure of the C-terminal region. *J. Biol. Chem.* 273: 34837–34842.
- Muller, M., Meijer, C., Zaman, G.J., Borst, P., Scheper, R.J., Mulder, N.H., de Vries, E.G. and Jansen, P.L. 1994. Overexpression of the gene encoding the multidrug resistance-associated protein results in increased ATP-dependent glutathione S-conjugate transport. *Proc. Natl. Acad. Sci. USA* 91: 13033–13037.
- Ohara, K., Kokado, Y., Yamamoto, H., Sato, F. and Yazaki, K. 2004. Engineering of ubiquinone biosynthesis using the yeast *coq2* gene confers oxidative stress tolerance in transgenic tobacco. *Plant J.* 40: 734–743.
- Pence, N.S., Larsen, P.B., Ebbs, S.D., Letham, D.L., Lasat, M.M., Garvin, D.F., Eide, D. and Kochian, L.V. 2000. The molecular physiology of heavy metal transport in the Zn/Cd hyperaccumulator *Thlaspi caerulescens*. *Proc. Natl. Acad. Sci. USA* 97: 4956–4960.
- Porra, R.J., Thompson, W.A. and Kriedemann, P.E. 1989. Determination of accurate extinction coefficients and simultaneous equations for assaying chlorophylls a and b extracted with four different solvents: verification of the concentration of chlorophyll standards by atomic absorption spectroscopy. *Biochim. Biophys. Acta* 975: 384–394.
- Renes, J., de Vries, E.G., Nienhuis, E.F., Jansen, P.L. and Muller, M. 1999. ATP- and glutathione-dependent transport of chemotherapeutic drugs by the multidrug resistance protein MRP1. *Br. J. Pharmacol.* 126: 681–688.
- Rajagopal, A. and Simon, S.M. 2003. Subcellular localization and activity of multidrug resistance proteins. *Mol. Biol. Cell* 14: 3389–3399.
- Saeki, T., Shimabuku, A.M., Ueda, K. and Komano, T. 1992. Specific drug binding by purified lipid-reconstituted P-glycoprotein: dependence on the lipid composition. *Biochim. Biophys. Acta* 1107: 105–110.
- Sato, F., Hashimoto, T., Hachiya, A., Tamura, K., Choi, K.B., Morishige, T., Fujimoto, H. and Yamada, Y. 2001. Metabolic engineering of plant alkaloid biosynthesis. *Proc. Natl. Acad. Sci. USA* 98: 367–372.
- Shitan, N., Bazin, I., Dan, K., Obata, K., Kigawa, K., Ueda, K., Sato, F., Forestier, C. and Yazaki, K. 2003. Involvement of CjMDR1, a plant multidrug-resistance-type ATP-binding cassette protein, in alkaloid transport in *Coptis japonica*. *Proc. Natl. Acad. Sci. USA* 100: 751–756.
- Skidmore, A.F. and Beebe, T.J. 1989. Characterization and use of the potent ribonuclease inhibitor aurintricarboxylic acid for the isolation of RNA from animal tissues. *Biochem. J.* 263: 73–80.
- Song, W.Y., Sohn, E.J., Martinoia, E., Lee, Y.J., Yang, Y.Y., Jasinski, M., Forestier, C., Hwang, I. and Lee, Y. 2003.

- Engineering tolerance and accumulation of lead and cadmium in transgenic plants. *Nat. Biotechnol.* 21: 914–919.
- Takeda, S., Sato, F., Ida, K. and Yamada, Y. 1990. Characterization of polypeptides that accumulate in cultured *Nicotiana tabacum* cells. *Plant Cell Physiol.* 31: 215–221.
- Terasaka, K., Blakeslee, J.J., Titapiwatanakun, B., Peer, W.A., Bandyopadhyay, A., Makam, S.N., Lee, O.R., Richards, E.L., Murphy, A.S., Sato, F. and Yazaki, K. 2005. PGP4, an ATP-binding cassette P-glycoprotein, catalyzes auxin transport in *Arabidopsis thaliana* roots. *Plant Cell* 17: 2922–2939.
- Theodoulou, F.L. 2000. Plant ABC transporters. *Biochim. Biophys. Acta* 1465: 79–103.
- Tommasini, R., Evers, R., Vogt, E., Mornet, C., Zaman, G.J., Schinkel, A.H., Borst, P. and Martinoia, E. 1996. The human multidrug resistance-associated protein functionally complements the yeast cadmium resistance factor 1. *Proc. Natl. Acad. Sci. USA* 93: 6743–6748.
- Tommasini, R., Vogt, E., Fromenteau, M., Hortensteiner, S., Matile, P., Amrhein, N. and Martinoia, E. 1998. An ABC transporter of *Arabidopsis thaliana* has both glutathione-conjugate and chlorophyll catabolite transport activity. *Plant J.* 13: 773–780.
- Vaucheret, H., Beclin, C. and Fagard, M. 2001. Post-transcriptional gene silencing in plants. *J. Cell Sci.* 114: 3083–3091.
- Verpoorte, R. and Memelink, J. 2002. Engineering secondary metabolite production in plants. *Curr. Opin. Biotechnol.* 13: 181–187.
- Wang, E., Wang, R., DeParasis, J., Loughrin, J.H., Gan, S. and Wagner, G.J. 2001. Suppression of a P450 hydroxylase gene in plant trichome glands enhances natural-product-based aphid resistance. *Nat. Biotechnol.* 19: 371–374.
- Yakura, K. and Tanifuji, S. 1983. Molecular cloning and restriction analysis of *EcoRI*-fragments of *Vicia faba* rDNA. *Plant Cell Physiol.* 24: 1327–1330.
- Yazaki, K. 2004. Natural products and metabolites. In: H. Klee and P. Christou (Eds.), *Handbook of Plant Biotechnology*, John Wiley & Sons Ltd, West Sussex, UK, pp. 811–857.
- Yazaki, K., Matsuoka, H., Shimomura, K., Bechthold, A. and Sato, F. 2001. A novel dark-inducible protein, LeDI-2, and its involvement in root-specific secondary metabolism in *Lithospermum erythrorhizon*. *Plant Physiol.* 125: 1831–1841.
- Zaman, G.J., Flens, M.J., van Leusden, M.R., de Haas, M., Mulder, H.S., Lankelma, J., Pinedo, H.M., Scheper, R.J., Baas, F., Broxterman, H.J. and Borst, P. 1994. The human multidrug resistance-associated protein MRP is a plasma membrane drug-efflux pump. *Proc. Natl. Acad. Sci. USA* 91: 8822–8826.
- Zhu, Y.L., Pilon-Smits, E.A., Tarun, A.S., Weber, S.U., Jouanin, L. and Terry, N. 1999. Cadmium tolerance and accumulation in Indian mustard is enhanced by overexpressing gamma-glutamylcysteine synthetase. *Plant Physiol.* 121: 1169–1178.

## Modulation of drug-stimulated ATPase activity of human MDR1/P-glycoprotein by cholesterol

Yasuhisa KIMURA\*, Noriyuki KIOKA\*, Hiroaki KATO†‡, Michinori MATSUO\* and Kazumitsu UEDA\*<sup>1</sup>

\*Laboratory of Cellular Biochemistry, Division of Applied Life Sciences, Kyoto University Graduate School of Agriculture, Kyoto 606-8502, Japan, †Department of Structural Biology, Kyoto University Graduate School of Pharmaceutical Sciences, Kyoto 606-8501, Japan, and ‡RIKEN Harima Institute at Spring-8, Hyogo 679-5148, Japan

MDR1 (multidrug resistance 1)/P-glycoprotein is an ATP-driven transporter which excretes a wide variety of structurally unrelated hydrophobic compounds from cells. It is suggested that drugs bind to MDR1 directly from the lipid bilayer and that cholesterol in the bilayer also interacts with MDR1. However, the effects of cholesterol on drug-MDR1 interactions are still unclear. To examine these effects, human MDR1 was expressed in insect cells and purified. The purified MDR1 protein was reconstituted in proteoliposomes containing various concentrations of cholesterol and enzymatic parameters of drug-stimulated ATPase were compared. Cholesterol directly binds to purified MDR1 in a detergent soluble form and the effects of cholesterol on drug-stimulated ATPase activity differ from one drug to another. The effects of cholesterol on  $K_m$  values of drug-stimulated ATPase activity were strongly correlated with the molecular mass of that drug. Cholesterol increases the binding affinity of small drugs

(molecular mass < 500 Da), but does not affect that of drugs with a molecular mass of between 800 and 900 Da, and suppresses that of valinomycin (molecular mass > 1000 Da).  $V_{max}$  values for rhodamine B and paclitaxel are also increased by cholesterol, suggesting that cholesterol affects turnover as well as drug binding. Paclitaxel-stimulated ATPase activity of MDR1 is enhanced in the presence of stigmasterol, sitosterol and campesterol, as well as cholesterol, but not ergosterol. These results suggest that the drug-binding site of MDR1 may best fit drugs with a molecular mass of between 800 and 900 Da, and that cholesterol may support the recognition of smaller drugs by adjusting the drug-binding site and play an important role in the function of MDR1.

**Key words:** cholesterol, drug-binding pocket, multidrug resistance, substrate recognition.

### INTRODUCTION

MDR1 (multidrug resistance 1; ABCB1) is a plasma membrane-located glycoprotein that confers multidrug resistance on cancer cells by actively excreting structurally diverse chemotherapeutic compounds from cells [1–4]. MDR1 is clinically important because it not only confers multidrug resistance but also affects the pharmacokinetics of various drugs [5–7].

MDR1 is a 1280-amino acid protein with two symmetrical halves connected by a short linker region [8]. Each half consists of six putative transmembrane helices followed by a nucleotide binding fold, in which ATP is hydrolysed to energize the transport. The hydrolysis is thought to be directly linked to drug transport and both nucleotide binding folds should be catalytically active [9,10], although the exact number of ATP molecules hydrolysed for a single transport is still unknown [11,12].

As structural information on MDR1 is limited, it is not known how MDR1 recognizes and transports such structurally diverse compounds. However, biochemical studies have revealed that MDR1 possesses multiple drug-binding sites [13–15] and these sites are located in the middle of the lipid bilayer [16]. Shapiro et al. [14] demonstrated that MDR1 possesses at least three positively co-operating drug-binding sites, an H site selective for Hoechst 33342 and colchicine, an R site selective for rhodamine 123 and anthracyclines, and another site at which progesterone binds. Drug-binding to one site stimulates transport by the other. Moreover, rhodamine 123 and progesterone in combination stimulate the transport of Hoechst 33342 in an additive manner.

Martin et al. [13] also assigned four drug-binding sites, three of which were classified as sites for transport and one for regulation of the transport.

Recently, many ABC (ATP-binding cassette) proteins have been reported to function in lipid homeostasis. For example, ABCG5 and ABCG8 mediate the efflux of cholesterol and sitosterol from the intestine and hepatocytes into the intestinal lumen and bile duct [17]. ABCA1 mediates the efflux of cholesterol and phospholipids to form high density lipoprotein [18–20]. ABCB4 (MDR2), being highly homologous with MDR1, functions in the secretion of PC (phosphatidylcholine) into bile ducts from hepatocytes [21]. Therefore it is conceivable that MDR1 also interacts with membrane lipids. Indeed, it has been reported that cholesterol stimulates basal (i.e. without any drugs) ATPase activity [22,23], and that cholesterol is recognized and transported as an endogenous substrate of MDR1 [24]. It was also shown that depletion of cholesterol reduced the transport activity of MDR1, resulting in the intracellular accumulation of drugs in cells [23,25,26].

In the present study, we analysed the ATPase activity of MDR1 using purified human MDR1 reconstituted in liposomes containing 0–20% (w/w) cholesterol. Cholesterol increased the basal ATPase activity and affected the drug-stimulated ATPase activity of MDR1. The effects differ from one drug to another and can be classified into five types. [<sup>3</sup>H]Cholesterol was co-eluted with MDR1 in a gel-filtration assay. These results suggest that cholesterol directly binds to MDR1 and modulates substrate recognition by MDR1.

Abbreviations used: ABC, ATP-binding cassette; c.m.c., critical micellar concentration; DDM, *N*-dodecyl- $\beta$ -D-maltoside; DTT, dithiothreitol; HEK, human embryonic kidney; KcsA, bacterial K<sup>+</sup> channel protein; M $\beta$ CD, methyl- $\beta$ -cyclodextrin; MDR1, multidrug resistance 1; Ni-NTA, Ni<sup>2+</sup>-nitrilotriacetate; PC, phosphatidylcholine; PE, phosphatidylethanolamine; PS, phosphatidylserine.

<sup>1</sup> To whom correspondence should be addressed (email uedak@kais.kyoto-u.ac.jp).

## EXPERIMENTAL

## Materials

Sf9 cells were obtained from Pharmingen. Lipids and ATP were purchased from Sigma–Aldrich. Medium, pluronic F-68 and gentamycin were obtained from Invitrogen. DDM (*N*-dodecyl- $\beta$ -D-maltoside) was purchased from Anatrace. Ni-NTA (Ni<sup>2+</sup>-nitrilotriacetate) agarose was from Qiagen. [ $1\alpha,2\alpha(n)^3$ H]Cholesterol was from Amersham Biosciences. Other compounds were from Sigma–Aldrich or Wako.

## Protein expression and purification

A sequence encoding a thrombin-cleavage site, ten histidine codons and a termination codon was inserted at the 3' end of human MDR1 cDNA [27]. The modified MDR1 was expressed in insect cells with the use of a recombinant baculovirus and purified by Ni-NTA chromatography as described in [28] with some modifications. The microsomal pellet was treated with 0.5 M NaCl before membrane proteins were solubilized with 0.8% (w/w) DDM to remove the peripherally anchored proteins as described elsewhere in detail (Kodan, A., Shibata, H., Matsumoto, T., Matsuo, M., Ueda, K. and Kato, K., unpublished work).

The N-terminus decahistidine-tagged KcsA expression vector was kindly provided by Dr Ichio Shimada (Graduate School of Pharmaceutical Sciences, University of Tokyo, Tokyo). His-tagged KcsA (bacterial K<sup>+</sup> channel protein) was expressed and purified according to a previously published report with minor modifications [29]. The *Escherichia coli* strain C41 was transformed with the expression plasmid and cultured in Luria–Bertani medium supplemented with 50 mg/l kanamycin. The protein expression was induced by the addition of 1 mM isopropyl  $\beta$ -D-thiogalactoside at  $D_{600} = 0.6$ . Cells were harvested at 6 h post-induction and disrupted by sonication. The membrane proteins were solubilized by PBS containing 1% DDM at room temperature (25 °C) and purified with Ni-NTA agarose. In the final step of purification, the detergent was replaced with 0.1% deoxycholate.

## Reconstitution into proteoliposomes

PC, PE (phosphatidylethanolamine), PS (phosphatidylserine) and cholesterol were dissolved in chloroform mixed in a proper ratio, and dried under high vacuum for over 2.5 h to remove the chloroform. The lipid film was resuspended at 10 mg/ml in 40 mM Tris/HCl (pH 7.4) and 0.1 mM EGTA by sonication in a bath sonicator (Bioruptor CD-200 TM, Cosmo Bio) until the suspension clarified. After sonication, lipids were kept on ice for 24 h and subjected to two cycles of freeze–thawing. Finally, lipids were sonicated again (5 cycles, 30 s each, 2 min rests on ice between cycles). Lipid stocks were used within a week. For reconstitution, purified protein and lipid stocks were mixed at a protein/lipid ratio of 1:10 and incubated at 23 °C for 20 min, and sonicated for 15 s in a bath sonicator as reported previously [28].

## MDR1 ATPase activity

The ATPase reaction was performed following methods reported previously [28] with minor modifications. Reconstituted protein (30–100 ng) was reacted in 20  $\mu$ l of 40 mM Tris/HCl (pH 7.5), 0.1 mM EGTA, 1 mM NaATP, 1 mM MgCl<sub>2</sub> and various concentrations of drugs at 37 °C for 30 min. The reaction was stopped by adding 10  $\mu$ l of 3% SDS and 10 mM vanadate.

## Enzymatic parameter

The experimental data were computer-fitted to the Michaelis–Menten equation,  $v = V_{Dmax}[S]/(K_m + [S])$ , where  $v$  is drug-stimu-

**Table 1**  $K_m$  and  $V_{max}$  values of drug-stimulated ATPase activity of MDR1 reconstituted in liposomes containing various concentrations of cholesterol

Purified MDR1 was reconstituted in liposomes of various concentrations of cholesterol and ATPase activity was examined in the presence of the indicated drugs. Data were fit to a Michaelis–Menten equation after subtracting the basal activity (0% cholesterol without drugs), and  $K_m$  or  $V_{max}$  values (which include the stimulation by cholesterol) were extracted. Values are means  $\pm$  S.D. ( $n = 3$ ). Relative values (percentage change) with respect to control (0% cholesterol) are shown in parentheses.

Drug	Molecular mass (Da)	Cholesterol (%)	$K_m$ ( $\mu$ M)	$V_{max}$ (nmol/min/mg)
Rhodamine 123	345	0	21 $\pm$ 2	874 $\pm$ 28
		5	16 $\pm$ 2 (76)	886 $\pm$ 45 (101)
		10	13 $\pm$ 1 (62)*	983 $\pm$ 24 (112)**
		20	10 $\pm$ 1 (48)*	757 $\pm$ 15 (87)**
Dexamethasone	392	0	826 $\pm$ 139	690 $\pm$ 67
		5	527 $\pm$ 88 (64)*	586 $\pm$ 68 (85)**
		10	423 $\pm$ 62 (51)*	620 $\pm$ 39 (90)**
		20	394 $\pm$ 3 (48)*	723 $\pm$ 23 (105)
Verapamil	455	0	4.1 $\pm$ 0.4	690 $\pm$ 24
		5	3.8 $\pm$ 0.3 (93)	637 $\pm$ 9 (92)*
		10	2.7 $\pm$ 0.0 (66)**	719 $\pm$ 4 (104)
		20	2.2 $\pm$ 0.2 (54)*	646 $\pm$ 12 (94)
Nicardipine	480	0	2.6 $\pm$ 0.2	568 $\pm$ 29
		5	1.5 $\pm$ 0.1 (58)**	596 $\pm$ 15 (105)
		10	1.6 $\pm$ 0.3 (62)*	634 $\pm$ 24 (112)*
		20	1.0 $\pm$ 0.2 (38)**	536 $\pm$ 16 (94)
Digoxin	781	0	181 $\pm$ 11	578 $\pm$ 20
		5	120 $\pm$ 8 (66)**	598 $\pm$ 2 (103)
		10	111 $\pm$ 20 (61)**	633 $\pm$ 26 (110)*
		20	76 $\pm$ 7 (42)**	576 $\pm$ 26 (100)
Rhodamine B	444	0	14 $\pm$ 3	233 $\pm$ 21
		5	9 $\pm$ 3 (64)*	291 $\pm$ 23 (125)*
		10	11 $\pm$ 1 (79)	305 $\pm$ 23 (131)*
		20	7 $\pm$ 1 (50)**	314 $\pm$ 3 (135)*
Vinblastine	811	0	1.7 $\pm$ 0.3	347 $\pm$ 5
		5	1.3 $\pm$ 0.1 (76)	368 $\pm$ 7 (106)*
		10	1.2 $\pm$ 0.1 (71)	304 $\pm$ 2 (88)**
		20	1.6 $\pm$ 0.3 (94)	297 $\pm$ 2 (86)**
Vincristine	825	0	3.7 $\pm$ 0.6	199 $\pm$ 20
		5	2.7 $\pm$ 0.4 (73)	307 $\pm$ 11 (154)**
		10	2.8 $\pm$ 0.4 (76)	215 $\pm$ 6 (108)
		20	3.9 $\pm$ 0.2 (105)	196 $\pm$ 6 (98)
Paclitaxel	854	0	1.4 $\pm$ 0.2	160 $\pm$ 10
		5	1.3 $\pm$ 0.1 (93)	235 $\pm$ 3 (147)**
		10	1.4 $\pm$ 0.1 (100)	363 $\pm$ 7 (227)**
		20	1.6 $\pm$ 0.2 (114)	411 $\pm$ 8 (257)**
Valinomycin	1111	0	2.5 $\pm$ 0.2	400 $\pm$ 2
		5	2.2 $\pm$ 0.1 (88)	408 $\pm$ 13 (102)
		10	2.6 $\pm$ 0.2 (104)	508 $\pm$ 7 (127)**
		20	3.5 $\pm$ 0.1 (140)**	418 $\pm$ 9 (105)

\*  $P < 0.05$  with respect to control (0% cholesterol).

\*\*  $P < 0.01$  with respect to control (0% cholesterol).

lated ATPase activity and  $[S]$  is the drug concentration. Fitting was carried out using the least-squares method (KaleidaGraph) and values for the  $V_{Dmax}$  and  $K_m$  were extracted.  $V_{max}$  values shown in Tables 1 and 2 include the drug-stimulated and sterol-stimulated ATPase activity. For  $V_{Dmax}$ ,  $v$  is the ATPase activity stimulated by drug alone. For  $V_{max}$ ,  $v$  is the ATPase activity stimulated by cholesterol and drug.

## In vitro cholesterol-binding assays

In vitro cholesterol-binding assays were carried out using size-exclusion chromatography and Ni-NTA pull-down assays were

**Table 2**  $K_m$  and  $V_{max}$  values of paclitaxel-stimulated ATPase activity of MDR1 reconstituted in liposomes containing various sterols (20%, w/w)

	$K_m$ ( $\mu$ M)	$V_{max}$ (nmol/min/mg)
–sterol	1.4 $\pm$ 0.2	160 $\pm$ 10
Cholesterol	1.6 $\pm$ 0.2	411 $\pm$ 8*
Stigmasterol	1.4 $\pm$ 0.1	379 $\pm$ 11*
Sitosterol	1.1 $\pm$ 0.2	325 $\pm$ 13*
Campesterol	1.0 $\pm$ 0.1*	300 $\pm$ 4*
Ergosterol	0.9 $\pm$ 0.1*	177 $\pm$ 3

\*  $P < 0.01$  with respect to control (–sterol).

conducted as previously reported [30,31] with some modifications. Cholesterol-M $\beta$ CD (methyl- $\beta$ -cyclodextrin) complexes were prepared by mixing 1 volume of ethanol-dissolved [ $^3$ H]cholesterol with 4.5 volumes of M $\beta$ CD at a molar ratio of 1:50 and incubating the mixture for more than 30 min at room temperature. For gel-filtration assays, purified MDR1 (6  $\mu$ g) in a 0.1% deoxycholate solution was mixed with cholesterol-M $\beta$ CD complexes in a final volume of 10  $\mu$ l of separation buffer [40 mM Tris/HCl (pH 7.4), 0.1% deoxycholate and 2 mM DTT (dithiothreitol)]. Samples were incubated at 37°C for 2 min and loaded on a column of Sephadex G100 (1 ml) pre-equilibrated in 40 mM Tris/HCl (pH 7.4) and 0.1% deoxycholate. Fractions (10  $\times$  100  $\mu$ l) were collected and analysed for radioactivity with a liquid-scintillation counter. MDR1 protein was visualized by silver staining after SDS/PAGE. For Ni-NTA pull-down assays, 6  $\mu$ g of purified protein was mixed with cholesterol-M $\beta$ CD complexes in a final volume of 10  $\mu$ l of reaction buffer [40 mM Tris/HCl (pH 7.4), 0.1% deoxycholate and 150 mM NaCl]. Samples were incubated at 37°C for 2 min and 20  $\mu$ l of Ni-NTA agarose was added. Proteins were eluted from Ni-NTA agarose by 500 mM imidazole after washing and analysed for radioactivity with a liquid-scintillation counter.

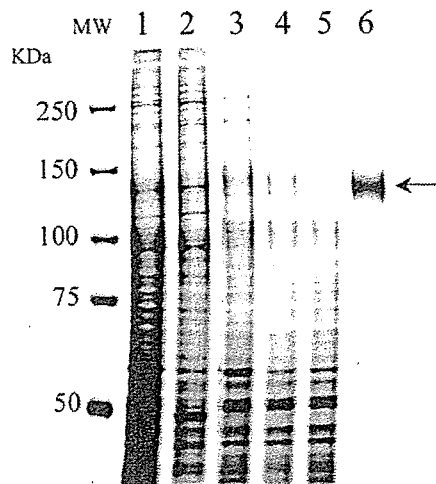
#### Expression of MDR1 in FreeStyle HEK (human embryonic kidney)-293F cells and analysis of ATPase activity

FreeStyle HEK-293F cells were cultured in Free Style 293 expression medium according to the manufacturer's instructions. Cells were transfected with the human MDR1 expression vector pCAGGSP/MDR1 (1  $\mu$ g/ml) [10] at a cell density of  $1.0 \times 10^6$ /ml and harvested 48 h after transfection. The membrane fraction (15  $\mu$ g of protein) was incubated in 20  $\mu$ l of PBS containing protease inhibitors, 1 mM EDTA and 10 mM M $\beta$ CD for 90 min at 25°C. The supernatant was removed after centrifugation (16 000 g for 5 min at room temperature), and the pellet was washed with PBS and subjected to ATPase analysis. To measure ATPase activity, the reaction was performed in 40 mM Tris/HCl (pH 7.5) containing 0.1 mM EGTA, 2 mM NaATP, 2 mM MgCl<sub>2</sub>, 2 mM DTT and 1 mM NaN<sub>3</sub> at 37°C for 30 min. ATPase activity was calculated by measuring inorganic phosphate as reported in [32].

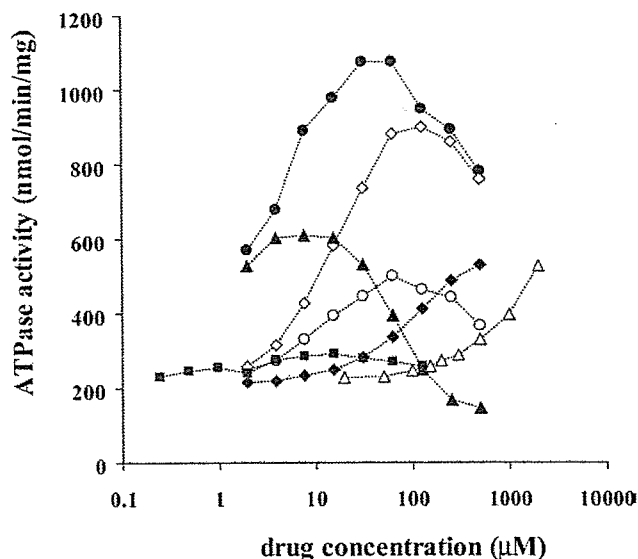
## RESULTS

### ATPase activity of purified human MDR1

Human MDR1, fused with a histidine tag at the C-terminus, was expressed at high levels in insect cells with an MDR1 recombinant baculovirus, and purified as previously reported [28]. MDR1 was extracted with 0.8% DDM, and purified by Ni-NTA affinity chromatography. MDR1 was recovered from the resin with 300 mM imidazole with a purity of more than 95% as judged from silver staining (Figure 1).

**Figure 1** Purification of human MDR1 expressed in insect cells

Aliquots from each step of purification were subjected to SDS/PAGE on an 8% polyacrylamide gel and visualized by silver staining. Lane 1, microsomal proteins from Sf9 cells expressing human MDR1; lane 2, peripheral proteins removed from microsomes by treatment with 0.5 M NaCl; lane 3, integral membrane proteins recovered after 0.5 M NaCl treatment; lane 4, microsomal proteins solubilized with 0.8% DDM; lane 5, proteins not bound to Ni-NTA resin; lane 6, eluate from Ni-NTA resin with 300 mM imidazole. Lanes 1–5, 2  $\mu$ g of protein was loaded; lane 6, 0.3  $\mu$ g of protein was loaded. MDR1 is indicated by the arrow.

**Figure 2** The effect of various drugs on the ATPase activity of purified MDR1

Purified MDR1 was reconstituted in PC/PE/PS (4:4:2) liposomes and ATPase activity was measured as described in the Experimental section. ●, Verapamil; ○, rhodamine B; ◇, digoxin; ◊, rhodamine 123; ▲, vinblastine; △, colchicine; ■, paclitaxel.

Purified MDR1 was reconstituted in liposomes (PC/PE/PS = 4:4:2), and ATPase activity was measured by HPLC with a titanium dioxide column [28]. Various compounds increased ATPase activity (Figure 2). A typical concentration-dependence with a bell-shaped curve [33,34] was obtained with verapamil and rhodamine 123; the ATPase activity increased as the concentration rose and peaked at about 30  $\mu$ M and 125  $\mu$ M respectively, whereas it was rather suppressed at higher concentrations. Vinblastine stimulated MDR1 ATPase activity at 10  $\mu$ M or less

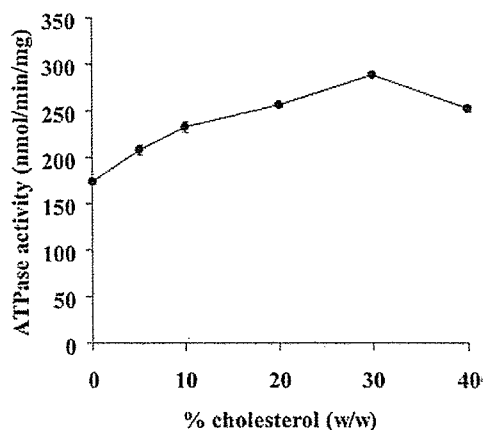


**Figure 3** Effects of cholesterol on the basal ATPase activity

Purified MDR1 was reconstituted in PC/PE/PS (4:4:2) liposomes containing 0, 5, 10, 20, 30 or 40% (w/w) cholesterol. Data are presented as means  $\pm$  S.D. ( $n=3$ ).

but showed strong inhibitory effects at higher concentrations and suppressed ATPase activity below the basal level (approx. 200 nmol/min/mg) at 200  $\mu$ M or more. With increasing concentration of colchicine there was an increase in ATPase, but maximal activity was not obtained even at 2 mM. Without the reconstitution in liposomes, ATPase activity was not stimulated by the addition of substrate drugs (results not shown), suggesting that the lipid environment is quite important for the function of MDR1 as reported previously [22].

#### Effects of cholesterol on MDR1 ATPase activity

It has been suggested that the basal ATPase activity of human MDR1 in native membrane vesicles is highly dependent on the presence of cholesterol [23,24], and also that the basal ATPase activity of partially purified hamster MDR1, reconstituted in PC/PE (9:1) liposomes, is dependent on the presence of cholesterol [22]. We examined whether cholesterol affects the ATPase activity of purified human MDR1 by reconstituting the protein in liposomes (PC/PE/PS = 4:4:2) containing various concentrations of cholesterol (Figure 3). The ATPase activity increased as the concentration of cholesterol increased and peaked at 30% (w/w) cholesterol. In the presence of 30% cholesterol, the ATPase activity of MDR1 was 1.7-fold greater than ATPase activity in the absence of cholesterol. This suggests that cholesterol directly interacted with MDR1 at drug-binding sites. Alternatively, cholesterol may have affected the lipid environment, fluidity for example, and indirectly increased the turnover of basal ATP hydrolysis.

#### Effects of various sterols on basal activity

To consider the possibility of an indirect effect of cholesterol on MDR1, the specificity of sterol species was examined (Figure 4). Stigmasterol, sitosterol and campesterol stimulated the MDR1 ATPase activity as efficiently as cholesterol. Ergosterol was less effective than other sterols. The specific effect of sterols on MDR1 ATPase activity may support the direct interaction of sterols with MDR1.

#### Binding of [ $^3$ H]cholesterol to detergent soluble MDR1

The direct binding of cholesterol to purified MDR1 was confirmed by two methods, a pull-down assay and size-exclusion chromatography. We found that a significant amount of chole-

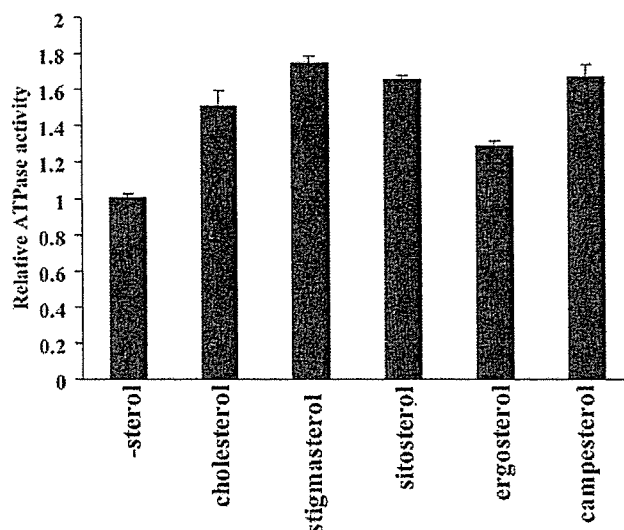


**Figure 4** Effects of sterols on the basal ATPase activity

Purified MDR1 was reconstituted in liposomes containing 20% (w/w) cholesterol, stigmasterol,  $\beta$ -sitosterol, ergosterol or campesterol. Relative ATPase activity is presented with respect to that in the absence of sterol (-sterol)  $\pm$  S.D. ( $n=3$ ).

sterol bound to micelles of DDM and eluted in earlier fractions (fractions 3–5) in both the absence and presence of MDR1. Thus, for the *in vitro* cholesterol binding assay, the detergent was replaced with 0.1% deoxycholate, which has a much higher c.m.c (critical micellar concentration) value and forms smaller micelles compared with those of DDM. MDR1 purified in 0.1% deoxycholate showed as much ATPase activity as that purified in DDM when reconstituted in proteoliposomes. Moreover, when MDR1 purified in 0.1% deoxycholate was reconstituted in liposomes containing 20% cholesterol, the  $K_m$  value for verapamil was decreased from  $4.7 \pm 0.4 \mu$ M to  $1.9 \pm 0.2 \mu$ M as discussed later (Table 1). These results suggest that MDR1 purified in deoxycholate is catalytically active and has similar features to MDR1 purified in DDM.

The Ni-NTA pull-down assay revealed that [ $^3$ H]cholesterol was co-precipitated with MDR1, but not with KcsA, whereas similar amounts of MDR1 and KcsA were precipitated (Figure 5A). To investigate further the binding of cholesterol to purified MDR1, size-exclusion chromatography was used. Soluble MDR1 was mixed with the cholesterol- $M\beta$ CD complex and loaded on to the column. When the cholesterol- $M\beta$ CD complex was mixed with MDR1, cholesterol was co-eluted with MDR1 (Figure 5B). In contrast, most cholesterol was retained in the column and was not eluted from Sephadex G100 resin when the cholesterol- $M\beta$ CD complex was applied to the column without MDR1, probably due to non-specific binding to the resin. The amount of cholesterol bound to MDR1 was correlated with the [ $^3$ H]cholesterol concentration and the amount of MDR1 (results not shown). Furthermore, the binding of [ $^3$ H]cholesterol to MDR1 was competitively inhibited by the unlabelled cholesterol- $M\beta$ CD complex (Figure 5C).

#### Effect of cholesterol on the drug-stimulated ATPase activity of MDR1

MDR1 has been suggested to possess multiple drug-binding sites, and a drug binding to one site allosterically modulates drugs binding to other sites [13–15]. Because the above results suggested that cholesterol interacts directly with MDR1, we

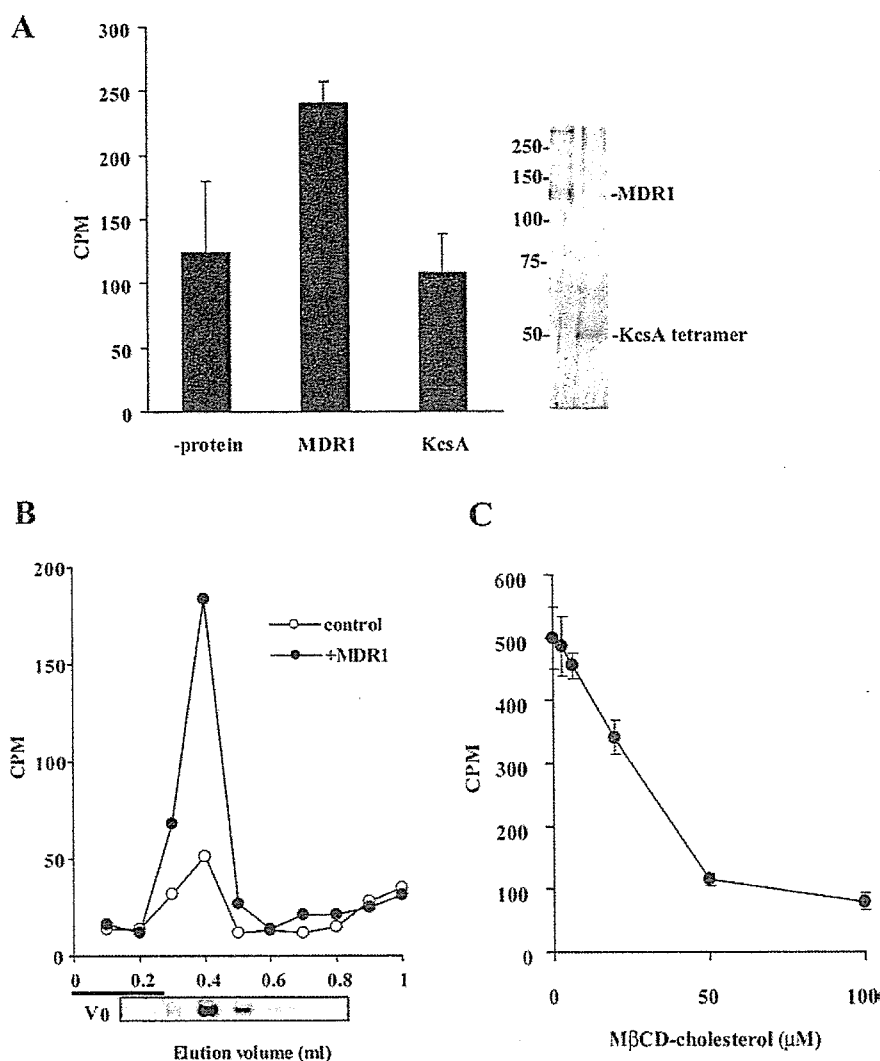


**Figure 5** Binding of cholesterol to purified MDR1

(A) Purified proteins (6  $\mu$ g) were mixed with 3  $\mu$ M of the [ $^3$ H]cholesterol-M $\beta$ CD complex at 37  $^{\circ}$ C for 2 min and Ni-NTA agarose was added. Proteins were eluted by 500 mM imidazole and analysed for radioactivity with a liquid-scintillation counter. Eluted protein was subjected to SDS/PAGE and visualized by silver-staining (right-hand panel). (B) Purified MDR1 (6  $\mu$ g) was mixed with 3  $\mu$ M [ $^3$ H]cholesterol-M $\beta$ CD complex at 37  $^{\circ}$ C for 2 min then loaded on a column of Sephadex G100 (1 ml) and each fraction (10  $\times$  100  $\mu$ l) was analysed for radioactivity with a liquid-scintillation counter. MDR1 protein was visualized by silver staining after SDS/PAGE. The column void volume is shown as  $V_0$ . (C) Competitive inhibition of [ $^3$ H]cholesterol with unlabelled cholesterol. Purified MDR1 was mixed with 3  $\mu$ M [ $^3$ H]cholesterol-M $\beta$ CD complex and unlabelled cholesterol-M $\beta$ CD complex. Fractions 3–6 were mixed and the amount of eluted [ $^3$ H]cholesterol was analysed.

expected cholesterol to affect the drug-stimulated ATPase activity of MDR1. We examined the drug-stimulated ATPase activity of MDR1 reconstituted either in liposomes (PC/PE/PS = 4:4:2) or in liposomes containing 20% (w/w) cholesterol. In the cases of rhodamine 123 and digoxin, the presence of cholesterol had little effect on the  $V_{max}$  of ATPase activity but significantly lowered the  $K_m$  value from 21 to 10  $\mu$ M (Figure 6A, Table 1) and from 181 to 76  $\mu$ M (Figure 6B, Table 1) respectively.

In contrast, the presence of cholesterol had little effect on the  $K_m$  for paclitaxel, but increased the  $V_{max}$  from 160 to 411 nmol/min/mg (Figure 6C, Table 1). These results suggested that cholesterol affected the drug-stimulated ATPase activity of MDR1 and effects of cholesterol differed from one drug to another: the presence of cholesterol increases the affinity of MDR1 for rhodamine 123 and digoxin, whereas it increases the paclitaxel-induced hydrolysis of ATP by MDR1.  $K_m$  values for ATP were

not affected by cholesterol in the absence or presence of paclitaxel (results not shown).

To further analyse effects of cholesterol on the drug-stimulated hydrolysis of ATP by MDR1, MDR1 was reconstituted in liposomes containing 0, 5, 10 or 20% (w/w) cholesterol and the enzymatic parameters of ATPase activity for ten drugs, rhodamine 123, verapamil, dexamethasone, digoxin, nifedipine, rhodamine B, paclitaxel, vinblastine, vincristine, and valinomycin, were examined (Table 1). The effects of cholesterol on  $K_m$  and  $V_{max}$  values of MDR1 ATPase activity differ from one drug to another as discussed later in the Discussion section.

#### Effect of cholesterol on steroid-stimulated ATPase activity of MDR1

We initially presumed that cholesterol would compete with dexamethasone at the shared binding site and increase the

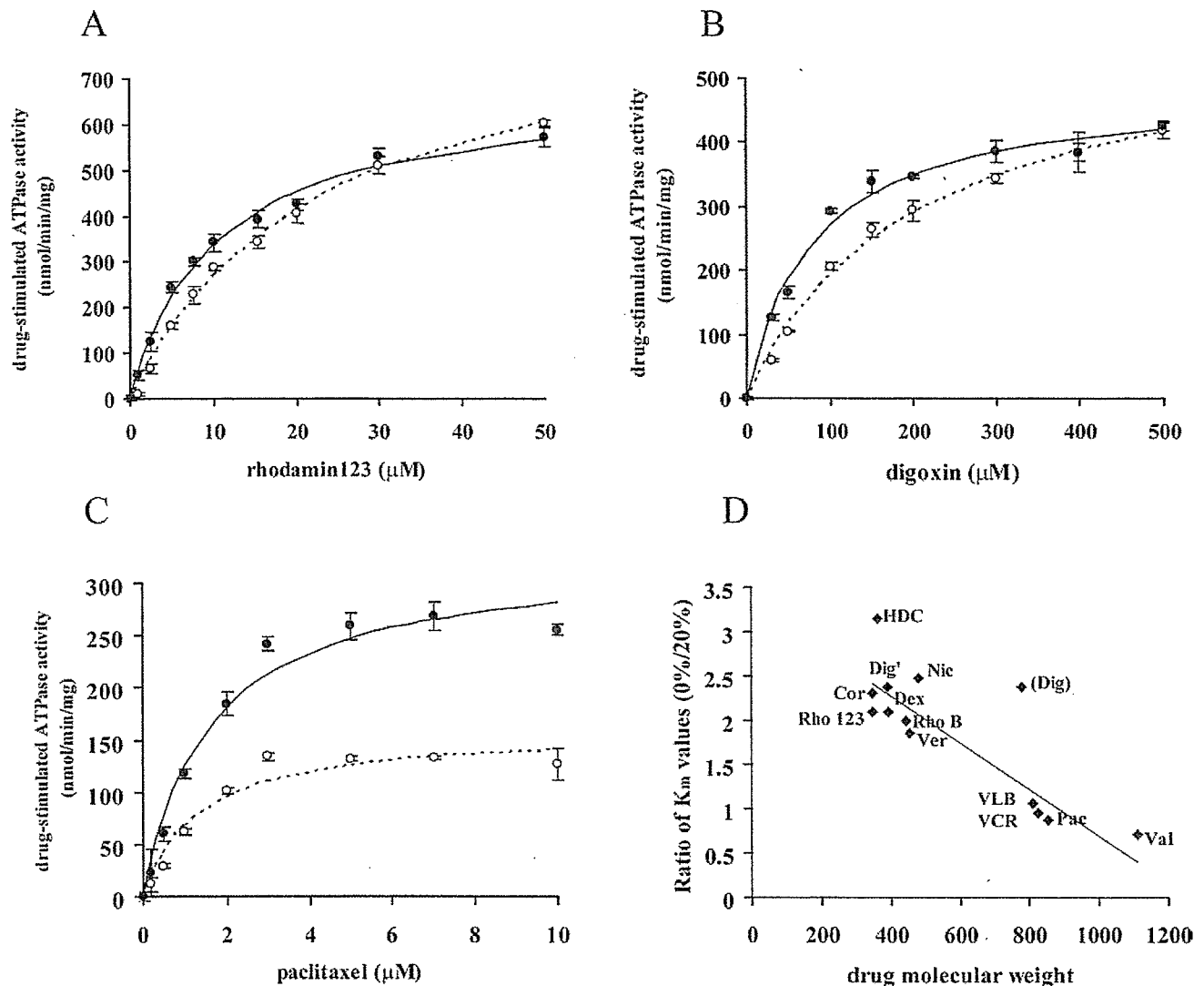


**Figure 6** The effect of cholesterol on drug-stimulated ATPase activity

Purified MDR1 reconstituted in liposomes containing 0% (open symbols) or 20% (filled symbols) cholesterol was reacted in the presence of various concentrations of drugs. (A) Rhodamine 123, (B) digoxin, and (C) paclitaxel. Experiments were performed in triplicate and means  $\pm$  S.D. are shown. After subtraction of the basal (without drug) activity, data were fitted to the Michaelis–Menten equation and  $K_m$  and  $V_{max}$  values were extracted. Lines represent calculated best-fit curves. (D) Relationship between the ratio of  $K_m$  values in the absence and presence of 20% (w/w) cholesterol and the molecular masses of drugs. The line represents the best fit linear regression ( $r^2 = 0.8075$ ; excluding the points for digoxin). Rho123, rhodamine 123; Cor, corticosterone; HDC, hydrocortisone; Dex, dexamethasone; Dig', aglycon form of digoxin; RhoB, rhodamine B; Ver, verapamil; Nic, nifedipine; Dig, digoxin; VLB, vinblastine; VCR, vincristine; Pac, paclitaxel; Val, valinomycin.

$K_m$  value for dexamethasone. However, as shown in Table 1, cholesterol decreased the  $K_m$  value for dexamethasone, indicating that the binding site for cholesterol is different from that for dexamethasone. To further examine the effect of cholesterol, we analysed effects on the ATPase activity of MDR1 stimulated by corticosterone and hydrocortisone (Figure 7).  $K_m$  values for both corticosterone and hydrocortisone decreased from 485  $\mu\text{M}$  to 210  $\mu\text{M}$  and from 1498  $\mu\text{M}$  to 475  $\mu\text{M}$  respectively when MDR1 was reconstituted in liposomes containing 20% cholesterol.

#### Effects of sterols on paclitaxel-stimulated ATPase activity of MDR1

Table 2 shows the effects of various sterols on the paclitaxel-stimulated ATPase activity of MDR1. Stigmasterol, sitosterol and campesterol as well as cholesterol increased the  $V_{max}$  value significantly. Ergosterol increased the  $V_{max}$  value slightly. On

the other hand, all of these sterols decreased the  $K_m$  value and increased the  $V_{max}$  value of the rhodamine B-stimulated ATPase activity of MDR1 as efficiently as cholesterol (results not shown). These results also suggest that the action of sterols is drug specific.

#### Effect of cholesterol depletion on drug-stimulated ATPase activity of MDR1 in mammalian cells

It has been reported that the depletion of membrane cholesterol significantly reduces the MDR1-mediated transport activity [23,26]. To investigate the role of cholesterol in the MDR1 ATPase activity in mammalian cells, we expressed MDR1 in FreeStyle HEK-293F cells and analysed the effect of cholesterol depletion on the verapamil-stimulated ATPase activity. With the depletion of cholesterol with 10 mM M $\beta$ CD, the  $K_m$  value for verapamil



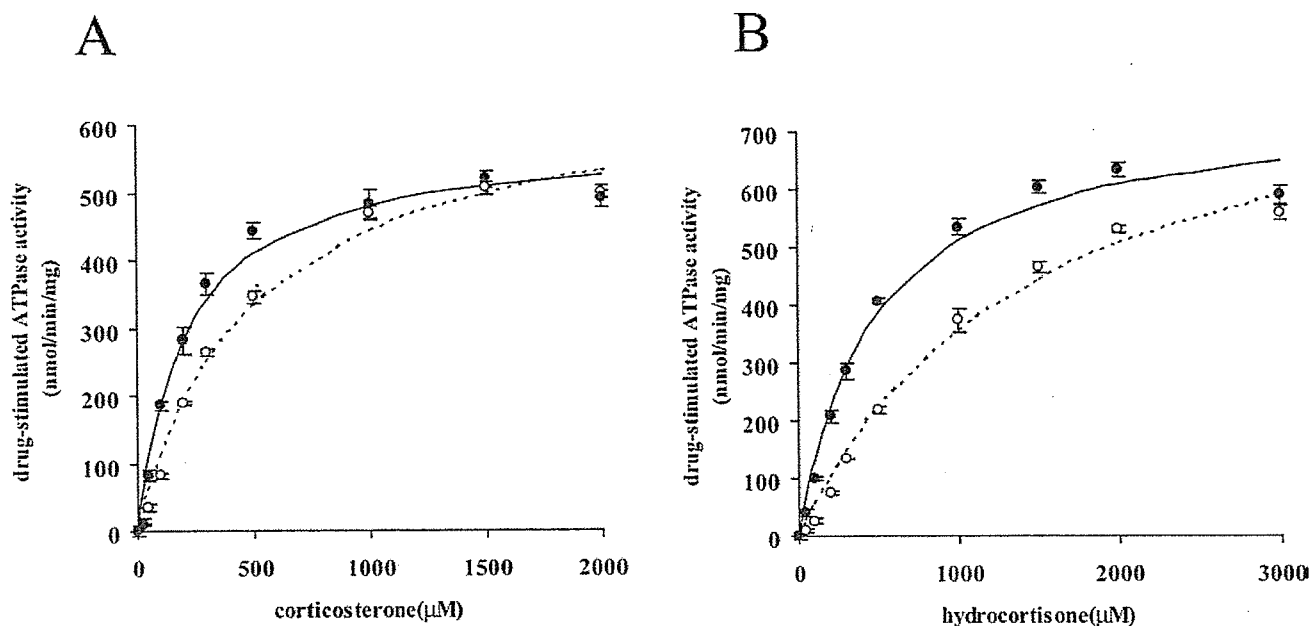


**Figure 7** Effects of cholesterol on corticosterone- and hydrocortisone-stimulated ATPase activity

Purified MDR1 reconstituted in liposomes containing 0% (open symbols) or 20% (filled symbols) cholesterol was reacted in the presence of corticosterone (A) or hydrocortisone (B). Experiments were performed in triplicate and means  $\pm$  S.D. are shown. Lines represent calculated best-fit curves.

shifted from  $3.2 \pm 0.8 \mu\text{M}$  to  $4.4 \pm 0.2 \mu\text{M}$ , although the  $V_{\text{max}}$  value was not reduced. This result suggests that the amount of cholesterol also affects the  $K_{\text{m}}$  value for drugs of MDR1 in native membranes, as observed in reconstituted liposomes.

## DISCUSSION

The results obtained in the present study demonstrate that cholesterol in membranes interacts directly with MDR1 and affects not only the basal ATPase activity but also the drug-stimulated ATPase activity of MDR1. Cholesterol affects both drug-binding ( $K_{\text{m}}$ ) and turnover of ATP hydrolysis ( $V_{\text{max}}$ ) of the purified human MDR1 reconstituted in liposomes. The effects of cholesterol differ from one drug to another and can be classified into five types depending on changes of kinetic parameters (Table 1). Type I involves rhodamine 123, dexamethasone, verapamil, nifedipine and digoxin: the  $K_{\text{m}}$  decreases in the presence of 20% cholesterol, but the  $V_{\text{max}}$  is little affected. Type II involves rhodamine B: the  $K_{\text{m}}$  decreases and the  $V_{\text{max}}$  increases in the presence of cholesterol. Type III involves vinblastine and vincristine: neither the  $K_{\text{m}}$  nor the  $V_{\text{max}}$  is affected greatly. Type IV involves paclitaxel: the  $K_{\text{m}}$  is not much affected and the  $V_{\text{max}}$  increases in the presence of cholesterol. Type V involves valinomycin: the  $K_{\text{m}}$  increases in the presence of cholesterol and the  $V_{\text{max}}$  is little affected.

The effects of cholesterol on the  $K_{\text{m}}$  were drug-specific. When the ratio of the  $K_{\text{m}}$  of each drug in the absence and presence of 20% cholesterol was plotted against the molecular mass of that drug, a strong correlation was found between them (Figure 6D). At first glance, digoxin did not fit the correlation, but when the aglycon form of digoxin (molecular mass 390 Da) was plotted on the graph, it fitted well. The binding affinity of drugs with a small molecular mass, between 350 and 500 Da, increased in the presence of 20% cholesterol, and these drugs (rhodamine 123, dexamethasone, verapamil, nifedipine, digoxin, corticosterone,

hydrocortisone and rhodamine B) are categorized into type I and type II (Table 1, Figure 6D). The binding affinity of drugs with a molecular mass of between 800 and 900 Da is not affected much by cholesterol, and these drugs (vinblastine, vincristine and paclitaxel) are categorized into type III and type IV. The binding affinity of valinomycin (type V), whose molecular mass is over 1000 Da, decreased in the presence of 20% cholesterol.

The effects of cholesterol might possibly arise indirectly, secondary to changes in the properties of the proteoliposomes such as permeability of the drugs or fluidity of the lipid bilayer. However, there are no correlations between hydrophobicity ( $\log P$  values) of drugs and the effects of cholesterol on either the  $K_{\text{m}}$  or  $V_{\text{max}}$  values. Cholesterol exerted various effects on the  $K_{\text{m}}$  in a drug-specific manner as described above, suggesting that those effects were caused by a direct interaction between MDR1 and cholesterol. The effects of cholesterol on the  $V_{\text{max}}$  values were also drug-specific. The  $V_{\text{max}}$  values for rhodamine B and paclitaxel are significantly increased in the presence of 20% cholesterol, whereas those for other drugs are not (Table 1). Moreover, the effects on  $V_{\text{max}}$  values of paclitaxel-stimulated ATPase activity are sterol-specific (Table 2). If the effects are thoroughly indirect, effects of cholesterol on drug-stimulated ATPase activity are expected to be observed for all the drugs. These results suggest that cholesterol affects the function of MDR1 by interacting with MDR1 directly, at least in part.

Modok et al. [35] showed that cholesterol alone does not alter the binding affinity for both nifedipine (molecular mass 480 Da) and XR9576 (molecular mass 647 Da). While these authors purified these proteins from drug-resistant Chinese-hamster ovary cells, in the present study we expressed and purified MDR1 in insect cells whose cholesterol content is quite low compared with that of mammalian cells [36]. This might affect the amount of cholesterol retained by the purified protein, which may cause the difference in the effects of exogenously added cholesterol.

The strong correlation between the effect of cholesterol on the  $K_{\text{m}}$  for drugs and their molecular masses suggests that the primary

effect of cholesterol could be on the drug-binding site. MDR1 has been suggested to possess several allosterically coupled drug-binding sites [13,14,37,38] and to bind more than one drug molecule at the same time [39,40]. Cholesterol may bind directly to or allosterically affect the drug-binding site to adjust its size for the drug. Because the binding affinity of drugs with a molecular mass of between 800 and 900 Da (vinblastine, vincristine and paclitaxel) is not affected by the presence of cholesterol, the drug-binding site of MDR1 may best fit drugs with these sizes. When small drugs, with a molecular mass of 350–500 Da, bind to MDR1, cholesterol (molecular mass 386.7 Da) may fill the empty space or allosterically tighten the drug-binding site and help in the recognition of smaller drugs.

We have previously demonstrated that the bulkiness of side chains at the position of His<sup>61</sup> and its neighbouring amino acid residues in the first transmembrane helix is important for substrate specificity [41,42]. For example, the replacement of His<sup>61</sup> by amino acids with bulkier side chains increased resistance to small drugs such as colchicine and VP16, while it lowered resistance to a large drug, vinblastine. Recently, it was also suggested that the first transmembrane helix forms part of the drug-binding pocket by cross-linking experiments using a thiol-reactive analogue of verapamil [43]. These observations also suggest that the size of the drug-binding pocket is important for recognizing drugs.

The most puzzling feature of MDR1 is its recognition of drugs with various structures and molecular masses, from 300 Da to well over 1000 Da. To function as an efflux pump for various lipophilic and toxic xenobiotics, it is necessary for MDR1 to recognize them as they pass through the lipid bilayer. Since substrate transport and ATP hydrolysis are tightly coupled, we have previously used purified human MDR1, reconstituted in liposomes, and measured the amounts of ADP released after the hydrolysis by HPLC with a titanium dioxide column [28]. Under our experimental conditions, the amount of detergent remaining in the ATPase reaction is less than 0.003%. This concentration is below the c.m.c. values of DDM (0.0087%), suggesting that reconstituted protein is embedded in the lipid bilayer. Moreover, the similar  $K_m$  values for verapamil in the native membrane (FreeStyle HEK-293F) and reconstituted proteoliposome suggest that the purified MDR1 is under native conditions as embedded in the plasma membrane. Inhibitors for other membrane-bound ATPases such as sodium azide and ouabain, which are necessary when membrane-bound or partially purified MDR1 is used in experiments [44,45], were not needed in the present study. These experimental conditions allowed us to examine the effect of cholesterol in the lipid bilayer on the MDR1 ATPase activity in detail. Because cholesterol is a major [about 20% (w/w) of lipids] and important constituent of the plasma membrane [46], liposomes containing cholesterol would provide more favourable conditions for MDR1. The highly sensitive ATPase assay established in the present study will not only facilitate our understanding of the drug-recognition mechanism of MDR1 but will also be useful for screening drugs interacting with MDR1.

In summary, we have analysed the ATPase activity and cholesterol-binding of MDR1 using purified human MDR1. The results suggest that cholesterol binds directly to MDR1 and modulates substrate-recognition by MDR1. The binding affinity of drugs with a small molecular mass increased in the presence of cholesterol. Cholesterol may fill the empty space or allosterically tighten the drug-binding site and aid the recognition of smaller drugs, and facilitate the ability of MDR1 to recognize compounds with various structures and molecular masses.

We thank Dr Tatsuya Kusudo for discussions. We also thank Dr Atsushi Kodan and Dr Vassilis Koronakis for advice on experimental procedures. This work was supported

by a Grant-in-aid for Scientific Research and Creative Scientific Research 15GS0301 from the Ministry of Education, Culture, Sports, Science and Technology, Ministry of Health, Labor and Welfare, Japan, the Association for the Progress of New Chemistry, and BRAIN (the Bio-oriented Technology Research Advancement Institution).

## REFERENCES

- Juliano, R. L. and Ling, V. (1976) A surface glycoprotein modulating drug permeability in Chinese hamster ovary cell mutants. *Biochim. Biophys. Acta.* **455**, 152–162
- Ueda, K., Cardarelli, C., Gottesman, M. M. and Pastan, I. (1987) Expression of a full-length cDNA for the human 'MDR1' gene confers resistance to colchicine, doxorubicin and vinblastine. *Proc. Natl. Acad. Sci. U.S.A.* **84**, 3004–3008
- Gottesman, M. M. and Pastan, I. (1993) Biochemistry of multidrug resistance mediated by the multidrug transporter. *Annu. Rev. Biochem.* **62**, 385–427
- Gottesman, M. M., Pastan, I. and Ambudkar, S. V. (1996) P-glycoprotein and multidrug resistance. *Curr. Opin. Genet. Dev.* **6**, 610–617
- Sparreboom, A., van Asperen, J., Mayer, U., Schinkel, A. H., Smit, J. W., Meijer, D. K., Borst, P., Noolen, W. J., Beijnen, J. H. and van Tellingen, O. (1997) Limited oral bioavailability and active epithelial excretion of paclitaxel (Taxol) caused by P-glycoprotein in the intestine. *Proc. Natl. Acad. Sci. U.S.A.* **94**, 2031–2035
- Ambudkar, S. V., Dey, S., Hrycyna, C. A., Ramachandra, M., Pastan, I. and Gottesman, M. M. (1999) Biochemical, cellular and pharmacological aspects of the multidrug transporter. *Annu. Rev. Pharmacol. Toxicol.* **39**, 361–398
- Greiner, B., Eichelbaum, M., Fritz, P., Kreichgauer, H. P., von Richter, O., Zundler, J. and Kroemer, H. K. (1999) The role of intestinal P-glycoprotein in the interaction of digoxin and rifampin. *J. Clin. Invest.* **104**, 147–153
- Chen, C. J., Chin, J. E., Ueda, K., Clark, D. P., Pastan, I., Gottesman, M. M. and Roninson, I. B. (1986) Internal duplication and homology with bacterial transport proteins in the *mdr1* (P-glycoprotein) gene from multidrug-resistant human cells. *Cell*, **47**, 381–389
- Urbatsch, I. L., Sankaran, B., Bhagat, S. and Senior, A. E. (1995) Both P-glycoprotein nucleotide-binding sites are catalytically active. *J. Biol. Chem.* **270**, 26956–26961
- Takada, Y., Yamada, K., Taguchi, Y., Kino, K., Matsuo, M., Tucker, S. J., Komano, T., Amachi, T. and Ueda, K. (1998) Non-equivalent cooperation between the two nucleotide-binding folds of P-glycoprotein. *Biochim. Biophys. Acta.* **14**, 131–136
- Ambudkar, S. V., Cardarelli, C. O., Pashinsky, I. and Stein, W. D. (1997) Relation between the turnover number for vinblastine transport and for vinblastine-stimulated ATP hydrolysis by human P-glycoprotein. *J. Biol. Chem.* **272**, 21160–21166
- Eytan, G. D., Regev, R. and Assaraf, Y. G. (1996) Functional reconstitution of P-glycoprotein reveals an apparent near stoichiometric drug transport to ATP hydrolysis. *J. Biol. Chem.* **271**, 3172–3178
- Martin, C., Berridge, G., Higgins, C. F., Mistry, P., Charlton, P. and Callaghan, R. (2000) Communication between multiple drug binding sites on P-glycoprotein. *Mol. Pharmacol.* **58**, 624–632
- Shapiro, A. B., Fox, K., Lam, P. and Ling, V. (1999) Stimulation of P-glycoprotein-mediated drug transport by prazosin and progesterone: evidence for a third drug-binding site. *Eur. J. Biochem.* **259**, 841–850
- Loo, T. W., Bartlett, M. C. and Clarke, D. M. (2003) Methanethiosulfonate derivatives of rhodamine and verapamil activate human P-glycoprotein at different sites. *J. Biol. Chem.* **278**, 50136–50141
- Loo, T. W. and Clarke, D. M. (2002) Location of the rhodamine-binding site in the human multidrug resistance P-glycoprotein. *J. Biol. Chem.* **277**, 44332–44338
- Yu, L., Hammer, R. E., Li-Hawkins, J., Von Bergmann, K., Lutjohann, D., Cohen, J. C. and Hobbs, H. H. (2002) Disruption of *Abcg5* and *Abcg8* in mice reveals their crucial role in biliary cholesterol secretion. *Proc. Natl. Acad. Sci. U.S.A.* **99**, 16237–16242
- Tanaka, A. R., Abe-Dohmae, S., Ohnishi, T., Aoki, R., Morinaga, G., Okuhira, K., Ikeda, Y., Kano, F., Matsuo, M., Kioka, N. et al. (2003) Effects of mutations of ABCA1 in the first extracellular domain on subcellular trafficking and ATP binding/hydrolysis. *J. Biol. Chem.* **278**, 8815–8819
- Lee, J. Y. and Parks, J. S. (2005) ATP-binding cassette transporter A1 and its role in HDL formation. *Curr. Opin. Lipidol.* **16**, 19–25
- Takahashi, K., Kimura, Y., Kioka, N., Matsuo, M. and Ueda, K. (2006) Purification and ATPase activity of human ABCA1. *J. Biol. Chem.* **281**, 10760–10768
- van Halbeert, A., Smith, A. J., Sprong, H., Fritzsche, I., Schinkel, A. H., Borst, P. and van Meer, G. (1996) MDR1 P-glycoprotein is a lipid translocase of broad specificity, while MDR3 P-glycoprotein specifically translocates phosphatidylcholine. *Cell*, **87**, 507–517
- Rothnie, A., Theron, D., Soceneantu, L., Martin, C., Traikia, M., Berridge, G., Higgins, C. F., Devaux, P. F. and Callaghan, R. (2001) The importance of cholesterol in maintenance of P-glycoprotein activity and its membrane perturbing influence. *Eur. Biophys. J.* **30**, 430–442

- 23 Gayet, L., Dayan, G., Barakat, S., Labialle, S., Michaud, M., Cogne, S., Mazane, A., Coleman, A. W., Rigal, D. and Baggetto, L. G. (2005) Control of P-glycoprotein activity by membrane cholesterol amounts and their relation to multidrug resistance in human CEM leukemia cells. *Biochemistry*, **44**, 4499–4509
- 24 Garrigues, A., Escargueil, A. E. and Orlowski, S. (2002) The multidrug transporter, P-glycoprotein, actively mediates cholesterol redistribution in the cell membrane. *Proc. Natl. Acad. Sci. U.S.A.* **99**, 10347–10352
- 25 Troost, J., Albermann, N., Emil Haefeli, W. and Weiss, J. (2004) Cholesterol modulates P-glycoprotein activity in human peripheral blood mononuclear cells. *Biochem. Biophys. Res. Commun.* **316**, 705–711
- 26 Troost, J., Lindenmaier, H., Haefeli, W. E. and Weiss, J. (2004) Modulation of cellular cholesterol alters P-glycoprotein activity in multidrug-resistant cells. *Mol. Pharmacol.* **66**, 1332–1339
- 27 Kioka, N., Tsubota, J., Kakehi, Y., Komano, T., Gottesman, M. M., Pastan, I. and Ueda, K. (1989) P-glycoprotein gene (MDR1) cDNA from human adrenal: normal P-glycoprotein carries Gly<sup>185</sup> with an altered pattern of multidrug resistance. *Biochem. Biophys. Res. Commun.* **162**, 224–231
- 28 Kimura, Y., Shibasaki, S., Morisato, K., Ishizuka, N., Minakuchi, H., Nakanishi, K., Matsuo, M., Amachi, T., Ueda, M. and Ueda, K. (2004) Microanalysis for MDR1 ATPase by high-performance liquid chromatography with a titanium dioxide column. *Anal. Biochem.* **326**, 262–266
- 29 Takeuchi, K., Yokogawa, M., Matsuda, T., Sugai, M., Kawano, S., Kohno, T., Nakamura, H., Takahashi, H. and Shimada, I. (2003) Structural basis of the KcsA K(+) channel and agitoxin2 pore-blocking toxin interaction by using the transferred cross-saturation method. *Structure*, **11**, 1381–1392
- 30 Hayward, R. D., Cain, R. J., McGhie, E. J., Phillips, N., Garner, M. J. and Koronakis, V. (2005) Cholesterol binding by the bacterial type III translocon is essential for virulence effector delivery into mammalian cells. *Mol. Microbiol.* **56**, 590–603
- 31 Radhakrishnan, A., Sun, L. P., Kwon, H. J., Brown, M. S. and Goldstein, J. L. (2004) Direct binding of cholesterol to the purified membrane region of SCAP: mechanism for a sterol-sensing domain. *Mol. Cell*, **15**, 259–268
- 32 Chifflet, S., Torriglia, A., Chiesa, R. and Tolosa, S. (1988) A method for the determination of inorganic phosphate in the presence of labile organic phosphate and high concentrations of protein: application to lens ATPases. *Anal. Biochem.* **168**, 1–4
- 33 Muller, M., Bakos, E., Welker, E., Varadi, A., Germann, U. A., Gottesman, M. M., Morse, B. S., Roninson, I. B. and Sarkadi, B. (1996) Altered drug-stimulated ATPase activity in mutants of the human multidrug resistance protein. *J. Biol. Chem.* **271**, 1877–1883
- 34 Loo, T. W. and Clarke, D. M. (1999) Identification of residues in the drug-binding domain of human P-glycoprotein: analysis of transmembrane segment 11 by cysteine-scanning mutagenesis and inhibition by dibromobimane. *J. Biol. Chem.* **274**, 35388–35392
- 35 Modok, S., Heyward, C. and Callaghan, R. (2004) P-glycoprotein retains function when reconstituted into a sphingolipid- and cholesterol-rich environment. *J. Lipid Res.* **45**, 1910–1918
- 36 Gimpl, G., Klein, U., Reilander, H. and Fahrenholz, F. (1995) Expression of the human oxytocin receptor in baculovirus-infected insect cells: high-affinity binding is induced by a cholesterol-cyclodextrin complex. *Biochemistry*, **34**, 13794–13801
- 37 Sharom, F. J., Yu, X., DiDiodato, G. and Chu, J. W. (1996) Synthetic hydrophobic peptides are substrates for P-glycoprotein and stimulate drug transport. *Biochem. J.* **320**, 421–428
- 38 Maki, N., Hafkemeyer, P. and Dey, S. (2003) Allosteric modulation of human P-glycoprotein: inhibition of transport by preventing substrate translocation and dissociation. *J. Biol. Chem.* **278**, 18132–18139
- 39 Dey, S., Ramachandra, M., Pastan, I., Gottesman, M. M. and Ambudkar, S. V. (1997) Evidence for two nonidentical drug-interaction sites in the human P-glycoprotein. *Proc. Natl. Acad. Sci. U.S.A.* **94**, 10594–10599
- 40 Loo, T. W., Bartlett, M. C. and Clarke, D. M. (2003) Simultaneous binding of two different drugs in the binding pocket of the human multidrug resistance P-glycoprotein. *J. Biol. Chem.* **278**, 39706–39710
- 41 Taguchi, Y., Morishima, M., Komano, T. and Ueda, K. (1997) Amino acid substitutions in the first transmembrane domain (TM1) of P-glycoprotein that alter substrate specificity. *FEBS Lett.* **413**, 142–146
- 42 Taguchi, Y., Kino, K., Morishima, M., Komano, T., Kane, S. E. and Ueda, K. (1997) Alteration of substrate specificity by mutations at the His<sup>61</sup> position in predicted transmembrane domain 1 of human MDR1/P-glycoprotein. *Biochemistry*, **36**, 8883–8889
- 43 Loo, T. W., Bartlett, M. C. and Clarke, D. M. (2006) Transmembrane segment 1 of human P-glycoprotein contributes to the drug binding pocket. *Biochem. J.* **396**, 537–545
- 44 Sarkadi, B., Price, E. M., Boucher, R. C., Germann, U. A. and Scarborough, G. A. (1992) Expression of the human multidrug resistance cDNA in insect cells generates a high activity drug-stimulated membrane ATPase. *J. Biol. Chem.* **267**, 4854–4858
- 45 al-Shawi, M. K. and Senior, A. E. (1993) Characterization of the adenosine triphosphatase activity of Chinese hamster P-glycoprotein. *J. Biol. Chem.* **268**, 4197–4206
- 46 Sprong, H., van der Sluijs, P. and van Meer, G. (2001) How proteins move lipids and lipids move proteins. *Nat. Rev. Mol. Cell. Biol.* **2**, 504–513

## Effect of Trimethoprim-Sulfamethoxazole on Na<sup>+</sup> and K<sup>+</sup> Transport Properties in the Rabbit Cortical Collecting Duct Perfused in vitro

Shigeaki Muto Shuichi Tsuruoka Yukio Miyata Akio Fujimura Eiji Kusano

Departments of Nephrology and Clinical Pharmacology, Jichi Medical School, Minamikawachi, Kawachi, Tochigi, Japan

### Key Words

Trimethoprim · Sulfamethoxazole · Hyperkalemia · Rabbit cortical collecting duct

### Abstract

**Background:** In this study, the membrane mechanisms of hyperkalemia caused by trimethoprim-sulfamethoxazole (TMP-SMX) combination antibiotics were assessed in the cortical collecting duct (CCD). **Methods:** We used the microelectrode technique and flux measurements, and examined the effects of TMP and SMX on electrical properties of the apical and basolateral membranes in the rabbit CCD perfused in vitro. **Results:** TMP in the lumen caused increases in apical membrane voltage, fractional apical membrane resistance ( $fR_A$ ), and transepithelial resistance ( $R_T$ ), all effects which were completely inhibited by luminal amiloride, but not by luminal Ba<sup>2+</sup>. The luminal TMP inhibited both net Na<sup>+</sup> reabsorption and K<sup>+</sup> secretion in the CCD. TMP in the bath slightly but significantly depolarized transepithelial voltage and basolateral membrane voltage without influencing  $fR_A$  or  $R_T$ . SMX in the lumen or bath had no effect on barrier voltages or resistances. **Conclusion:** TMP mainly acts on the apical membrane of the CCD, inhibits the amiloride-sensitive macroscopic Na<sup>+</sup> conductance in this membrane, and thereby decreases the net driving force for K<sup>+</sup> exit across the membrane, resulting in an inhibition of K<sup>+</sup> secretion. SMX in the lumen or bath had no effect on the CCD.

### Introduction

The trimethoprim-sulfamethoxazole (TMP-SMX) combination antibiotics is an extremely common medication given for treatment of a variety of infections. The adverse effect of hyperkalemia has been reported in acquired immunodeficiency syndrome patients 7–10 days after the start of high doses of TMP-SMX therapy for treatment of *Pneumocystis carinii* pneumonia [1–3] and in hospitalized patients treated with standard doses of TMP-SMX [4]. The hyperkalemia appears to be reversible as it ameliorates after withdrawal of the drug [1, 2].

The mechanisms for the hyperkalemia caused by TMP-SMX have not fully been understood, but the renin-angiotensin-aldosterone axis appears to be intact in most, but not all, cases [5, 6]. Fonseca et al. [7] reported that TMP inhibits Na<sup>+</sup> transport across the frog skin and competes with amiloride for blockade of Na<sup>+</sup> conductance. Velázquez et al. [8] described that TMP, when acutely infused into rats, caused a natriuresis and a fall in urinary K<sup>+</sup> excretion. They also observed that, in rat distal tubule perfused in vivo, addition of TMP to the luminal perfusate decreased net K<sup>+</sup> secretion and lumen-negative transepithelial voltage ( $V_T$ ), and speculated that TMP may impair Na<sup>+</sup> transport in the distal tubule and reduces lumen-negative  $V_T$  by the Na<sup>+</sup> transport, thereby decreasing the electrical gradient favoring passive K<sup>+</sup> secretion. However, they did not directly demonstrate it, because TMP had no effect on net Na<sup>+</sup> reabsorption in the distal tubule [8]. Because the distal tubule is composed of

Copyright © 2006 S. Karger AG, Basel

### KARGER

Fax +41 61 306 12 34  
E-Mail karger@karger.ch  
www.karger.com© 2006 S. Karger AG, Basel  
1660-2137/06/1024-0051\$23.50/0Accessible online at:  
www.karger.com/nepDr. Shigeaki Muto  
Department of Nephrology, Jichi Medical School  
Minamikawachi, Kawachi  
Tochigi 329-0498 (Japan)  
Tel. +81 285 58 7346, Fax +81 285 44 4869, E-Mail smuto@jichi.ac.jp

heterogeneous cells such as distal convoluted tubule cells, connecting tubule cells, principal collecting duct (CD) cells, and  $\alpha$ -intercalated cells [9], which cell(s) contribute(s) to the TMP-induced electrical changes remains unknown. In an A6 cell line derived from *Xenopus laevis* distal nephron, a model of mammalian cortical collecting duct (CCD) CD cell, Choi et al. [1] have shown that the apical TMP, but not the basolateral TMP, inhibited amiloride-sensitive short circuit current. Schlanger et al. [10] applied cell-attached patch clamp techniques to the A6 cell monolayers and reported that TMP acted from the apical membrane, and inhibited highly selective  $\text{Na}^+$  channel activity. However, it is not known whether TMP actually inhibits macroscopic  $\text{Na}^+$  conductance at the apical membrane of the intact mammalian CD cell and reduces net  $\text{Na}^+$  reabsorption and  $\text{K}^+$  secretion in the CCD. It is also possible that TMP may interact with SMX, and as a consequence may inhibit apical membrane  $\text{Na}^+$  conductance. Furthermore, there is a question as to whether TMP may directly act on the apical  $\text{K}^+$  conductance. In addition, Eiam-Ong et al. [11] reported a decrease in  $\text{Na}^+$ - $\text{K}^+$ -ATPase activity in the rat CCD, a finding that may also be able to account for the TMP-induced hyperkalemia. However, whether TMP directly influences basolateral  $\text{Na}^+$ - $\text{K}^+$  pump activity in the CCD is unclear. The above-mentioned reports suggest that TMP may act on both apical and basolateral membranes of the CD cell; however, which action contributes to the TMP-induced hyperkalemia remains unknown.

Therefore, the purpose of the present study was to determine the cellular and membrane mechanisms for the TMP-SMX-induced hyperkalemia. For this purpose, we examined the effects of TMP and SMX in the lumen and bath on electrical properties in the apical and basolateral membranes of the CD cell in isolated perfused CCDs from rabbit kidneys. We also examined the effects of TMP in the lumen on net transepithelial fluxes of  $\text{Na}^+$  and  $\text{K}^+$  in CCDs perfused in vitro.

## Methods

### Isolation and Perfusion of Tubules

Japanese female white rabbits (1.5–2.5 kg) were maintained on a standard rabbit chow and tap water ad libitum. The animals were anesthetized with intravenous sodium pentobarbital (35 mg/kg) and both kidneys were removed. Thin slices (1–2 mm) were cut from the coronal section of each kidney and transferred to a dish containing dissecting solution composed of (in mM): 14 KCl, 44  $\text{K}_2\text{HPO}_4$ , 14  $\text{KH}_2\text{PO}_4$ , 9  $\text{NaHCO}_3$  and 160 sucrose, a medium that had been shown to improve the quality of the kidney tissue [12–16]. The CCD was dissected and transferred to a bath chamber mounted on an

inverted microscope (Diaphot; Nikon, Tokyo, Japan). Methods used to perfuse the CCD have been described previously in our laboratory [12–15]. Briefly, after suspending the tubule between two pipettes, the lumen was perfused at a rate exceeding 20 nl/min. The distal end of the CCD was held in a collecting pipette coated with unpolymerized Sylgard 184 (Dow Corning Corp., Midland, Mich., USA). The volume of the bath chamber was  $\sim 100 \mu\text{l}$  to permit rapid exchange of different bath solutions within 5 s. The bath solution flowed by gravity at a rate of 5–15 ml/min from the reservoirs through a water jacket to stabilize the bath temperature at XXX.

### Electrical Measurements

The transepithelial and cellular electrical potentials were measured using methods described previously [12–15]. Briefly, transepithelial voltage ( $V_T$ ) was measured through the perfusion pipette, which was connected to one channel of a dual electrometer (Duo 773; W-P Instruments, Inc., Sarasota, Fla., USA) with a 3 M KCl-3% agar bridge and a calomel half-cell electrode. Bathing fluid was also connected through a 3 M KCl-3% agar bridge connected to another calomel half-cell electrode. Constant-current pulses ( $\Delta I$ ) (50 nA, 1 s in duration, and 10-second intervals) were injected into the tubule lumen via the perfusion pipette connected to a pulse generator (SEN-3301; Nihon Kohden, Tokyo, Japan). The voltage deflection at the perfusion end of the tubule ( $\Delta V_P$ ) was recorded via 3 M KCl-3% agar bridge and the electrometer noted above. The voltage deflection at the distal end of the tubule ( $\Delta V_D$ ) was also measured via a 3 M KCl-3% agar bridge inserted into the collecting pipette, which was connected to another electrometer (MEZ-7200; Nihon Kohden). The basolateral membrane voltage ( $V_B$ ) was measured with 0.5 M KCl-filled microelectrodes, which were fabricated from borosilicate glass capillaries (GD-1.5; 1.5 mm OD, 1.0 mm ID; Narishige Scientific Laboratory, Tokyo, Japan) by using a vertical puller (PE-2; Narishige Scientific Laboratory). They were fixed to a microelectrode holder containing an Ag-AgCl pellet and connected to another channel of a dual electrometer (Duo 773; W-P Instruments). To impale a tubular cell, a microelectrode was positioned against the basolateral membrane with a hydraulic micro-manipulator (WR-6; Narishige Scientific Laboratory) fixed to the stage of a microscope (Diaphoto, Nikon). The microelectrode was advanced into the cell by tapping the air-cushioned table. Both  $V_T$  and  $V_B$  were referenced to the bath and were recorded on a four-pen chart recorder (R64; Rikadenki, Tokyo, Japan). The electrical potential difference across the apical membrane ( $V_A$ ) was calculated as  $V_A = V_T - V_B$ . The length constant ( $\lambda$ ) was determined by

$$L/\lambda = \cosh^{-1} (\Delta V_P/\Delta V_D),$$

where  $L$  is the tubular length.  $R_T$  is obtained from the following equation [12–15]:

$$R_T = 2\pi r\lambda (\Delta V_P/\Delta I) \tanh (L/\lambda),$$

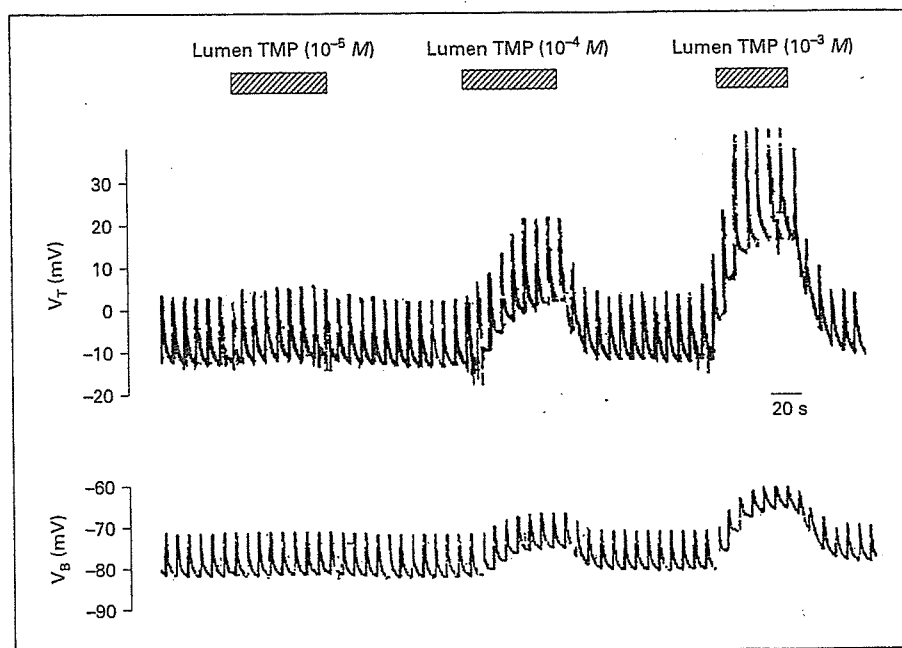
where  $r$  is the optical radius of the tubule. The fractional apical membrane resistance ( $fR_A$ ) was estimated as the following equation [12–15]:

$$fR_A = (\Delta V_x - \Delta V_B)/\Delta V_x,$$

where  $\Delta V_B$  and  $\Delta V_x$  are the current-induced voltage deflection of the  $V_B$  and the deflection of the  $V_T$  at the point of the microelectrode impalement, respectively. The  $\Delta V_x$  was estimated as

$$\Delta V_x = \Delta V_P \cosh (x/\lambda - L/\lambda)/\cosh (L/\lambda),$$

**Fig. 1.** Typical tracings showing effects of TMP at  $10^{-5}$ ,  $10^{-4}$ , and  $10^{-3}$  M in the lumen on  $V_T$  and  $V_B$  in the CCD. Voltage spikes are due to 50 nA constant-current pulses at 10-second intervals.



where  $x$  is the distance from the tip of the perfusion pipette to the point of cell impalement. The electrical radius calculated from the volume resistivity of the luminal perfusate and core resistance coincided with the optical radius within the range of variability of the measurements.

In the present experiments, only CD cells in the rabbit CCD were impaled, using methods of identification previously described [12–15].

#### Measurements of Net Transepithelial $\text{Na}^+$ and $\text{K}^+$ Fluxes

Net transepithelial water flux ( $J_V$ , nl/mm/min) was calculated as  $J_V = V_o (C^*_o/C^*_i - 1)/L$ , where  $V_o$  is the fluid collected rate (nl/min),  $L$  is the tubular length (mm),  $C^*_o$  and  $C^*_i$  are concentrations of  $^{14}\text{C}$ -methoxy inulin (New England Nuclear, Boston, Mass., USA) of the collected fluid and the luminal perfusate, respectively [16, 17]. The values of  $J_V$  greater than  $\pm 0.1$  nl/mm/min were assumed to represent water movement, including mechanical leaks, and were discarded. Net transepithelial fluxes of  $\text{Na}^+$  and  $\text{K}^+$  were determined by measuring concentrations of the luminal perfusate and collected fluid with a continuous flow fluorometer (Nanoflo; W-P Instruments) [17] and an ultramicro flame photometer (AFA-707-D; APEL, Saitama, Japan) [16], respectively. The net transepithelial fluxes of the solute  $X$  ( $J_X$ , pEq/mm/min) were calculated according to the equation:  $J_X = ([X]_i - [X]_o) V_o/L$ , where  $[X]_i$  and  $[X]_o$  are concentrations of the solute  $X$  in the luminal perfusate and the collected fluid, respectively. Negative value of  $J_X$  indicates net secretion. For the flux studies, the luminal flow rate was adjusted to  $\sim 7$  nl/min by regulating the hydrostatic perfusion pressure. Each reported flux represents the difference between three paired samples of the luminal perfusate and collected fluid with each sample measured in triplicate.

#### Solutions and Materials

The composition of the bathing and luminal solution used in this study was as follows (in mM): 110 NaCl, 5 KCl, 25  $\text{NaHCO}_3$ , 0.8  $\text{Na}_2\text{HPO}_4$ , 0.2  $\text{NaH}_2\text{PO}_4$ , 10 sodium acetate, 1.8  $\text{CaCl}_2$ , 1.0  $\text{MgCl}_2$ , 8.3  $d$ -glucose, and 5  $L$ -alanine. The pH of the solution was maintained at 7.4 by bubbling with 95%  $\text{O}_2$  and 5%  $\text{CO}_2$  gas, and the osmolality of the solution was between 285 and 295 mosm/kg  $\text{H}_2\text{O}$ .

Amiloride (Sigma Chemicals, St. Louis, Mo., USA) was added to the luminal perfusate to achieve a final concentration of 50  $\mu\text{M}$ .  $\text{BaCl}_2$  was used in the lumen at a final concentration of 2 mM. TMP, which was supplied by Shionogi & Co., Ltd. (Osaka, Japan), and SMX (Sigma) were dissolved in DMSO at 0.1% final concentrations. Equivalent concentrations of vehicle were added as a control for individual protocols.

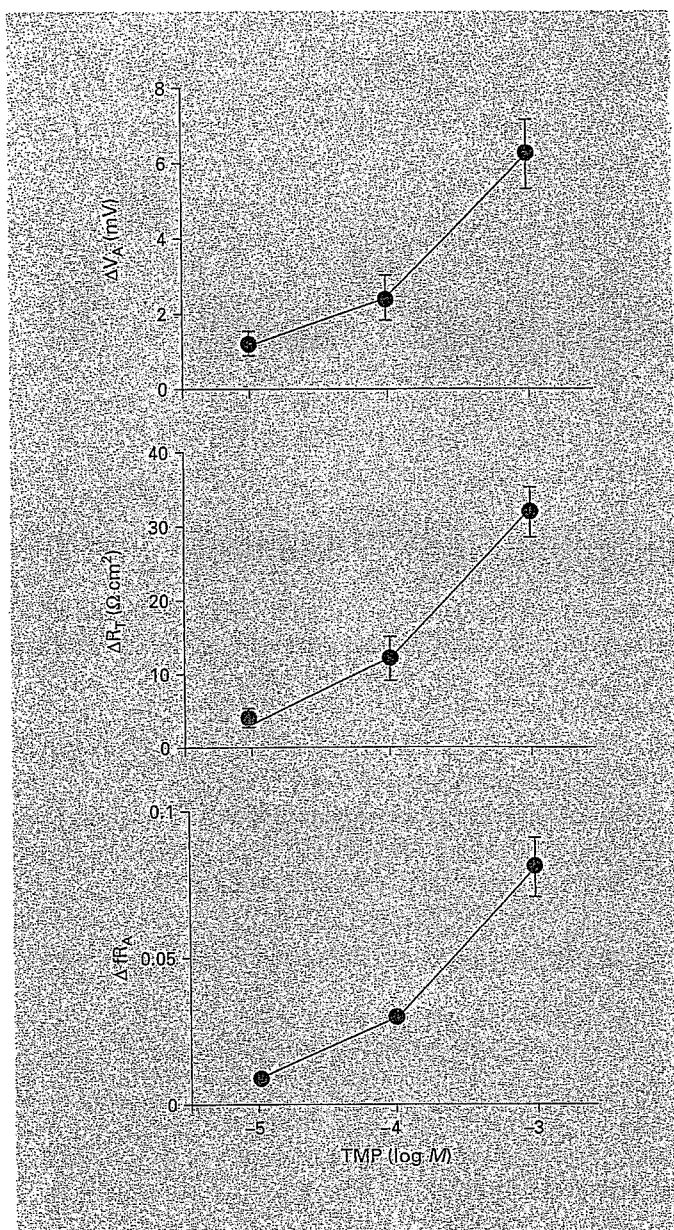
#### Statistics

Data are shown as means  $\pm$  SEM, and paired Student's  $t$  test was used to determine the significance of difference between successive measurements carried out on the same tubules. Statistical significance was taken as  $p < 0.05$ .

## Results

#### General Data

The CCD segments used in this study had an average length of  $904.8 \pm 36.4$   $\mu\text{m}$  ( $n = 23$ ). The optical inside diameter of these tubules was  $26.8 \pm 0.6$   $\mu\text{m}$  ( $n = 23$ ). The  $V_T$  averaged  $-8.5 \pm 0.8$  mV ( $n = 23$ ). The mean values of the  $R_T$  and length constant were  $114.5 \pm 2.0$   $\Omega \text{cm}^2$



( $n = 23$ ) and  $355.6 \pm 13.3 \mu\text{m}$  ( $n = 23$ ), respectively. These general data confirmed well with our previous reports [12–15].

#### Effect of TMP and SMX in the Lumen on Electrical Properties of the CD Cell

At first, we examined whether TMP acts directly on the apical membrane of the CD cell. For this purpose, we added TMP at  $10^{-5}$ ,  $10^{-4}$  and  $10^{-3} M$  to the luminal perfusate, and measured barrier voltages and resistances in the CCD. Figure 1 shows the effects of TMP at  $10^{-5}$ ,  $10^{-4}$ , and  $10^{-3} M$  in the lumen on  $V_T$  and  $V_B$ . Table 1 summarizes barrier voltages and resistances in the absence and presence of lumen TMP at  $10^{-5}$  up to  $10^{-3} M$ . TMP at  $10^{-5} M$  in the lumen significantly depolarized  $V_T$  from  $-11.7 \pm 2.3$  to  $-10.5 \pm 2.1$  mV ( $p < 0.01$ ) but had no effect on  $V_B$ , leading to a significant hyperpolarization of  $V_A$  from  $70.9 \pm 1.7$  to  $72.1 \pm 1.8$  mV ( $p < 0.05$ ). The  $R_T$  and  $fR_A$  significantly increased from  $118.7 \pm 4.4$  to  $122.6 \pm 5.1 \Omega \text{cm}^2$  ( $p < 0.005$ ) and from  $0.46 \pm 0.09$  to  $0.47 \pm 0.09$  ( $p < 0.005$ ), respectively. TMP at  $10^{-4} M$  in the lumen rapidly depolarized  $V_T$  and  $V_B$  from  $-11.3 \pm 2.1$  to  $-3.1 \pm 1.8$  mV ( $p < 0.001$ ) and from  $-81.9 \pm 1.7$  to  $-76.0 \pm 1.9$  mV ( $p < 0.005$ ), respectively, resulting in a significant hyperpolarization of  $V_A$  from  $70.5 \pm 1.6$  to  $72.9 \pm 1.8$  mV ( $p < 0.01$ ). The  $R_T$  and  $fR_A$  significantly increased from  $118.7 \pm 4.0$  to  $131.1 \pm 6.1 \Omega \text{cm}^2$  ( $p < 0.005$ ) and from  $0.46 \pm 0.09$  to  $0.49 \pm 0.09$  ( $p < 0.001$ ), respectively. When TMP at  $10^{-3} M$  was added to the luminal perfusate, the  $V_T$  and  $V_B$  rapidly depolarized from

**Fig. 2.** The concentration-response relationship for luminal addition of TMP on increases in  $V_A$ ,  $R_T$ , and  $fR_A$  ( $\Delta V_A$ ,  $\Delta R_T$ , and  $\Delta fR_A$ , respectively). Each point represents mean  $\pm$  SE of 8 separate experiments.

**Table 1.** Effects of TMP at  $10^{-5}$ ,  $10^{-4}$ , and  $10^{-3} M$  in the lumen on barrier voltages and resistances in the CCD

	Control	TMP ( $10^{-5} M$ )	Control	TMP ( $10^{-4} M$ )	Control	TMP ( $10^{-3} M$ )
$V_T$ , mV	$-11.7 \pm 2.3$	$-10.5 \pm 2.1^{**}$	$-11.3 \pm 2.1$	$-3.1 \pm 1.8^{++}$	$-10.9 \pm 1.9$	$9.3 \pm 2.7^{++}$
$V_B$ , mV	$-82.6 \pm 1.9$	$-82.6 \pm 1.7$	$-81.9 \pm 1.7$	$-76.0 \pm 1.9^+$	$-81.0 \pm 1.3$	$-67.0 \pm 2.9^+$
$V_A$ , mV	$70.9 \pm 1.7$	$72.1 \pm 1.8^*$	$70.5 \pm 1.6$	$72.9 \pm 1.8^{**}$	$70.1 \pm 2.1$	$76.3 \pm 2.2^{++}$
$R_T$ , $\Omega \text{cm}^2$	$118.7 \pm 4.4$	$122.6 \pm 5.1^+$	$118.7 \pm 4.0$	$131.1 \pm 6.1^+$	$119.1 \pm 4.8$	$151.0 \pm 6.6^{++}$
$fR_A$	$0.46 \pm 0.09$	$0.47 \pm 0.09^+$	$0.46 \pm 0.09$	$0.49 \pm 0.09^{++}$	$0.45 \pm 0.09$	$0.53 \pm 0.09^{++}$

Data are mean  $\pm$  SE of 8 tubules. \*  $p < 0.05$ , \*\*  $p < 0.01$ , +  $p < 0.005$ , ++  $p < 0.001$  compared with preceding period.



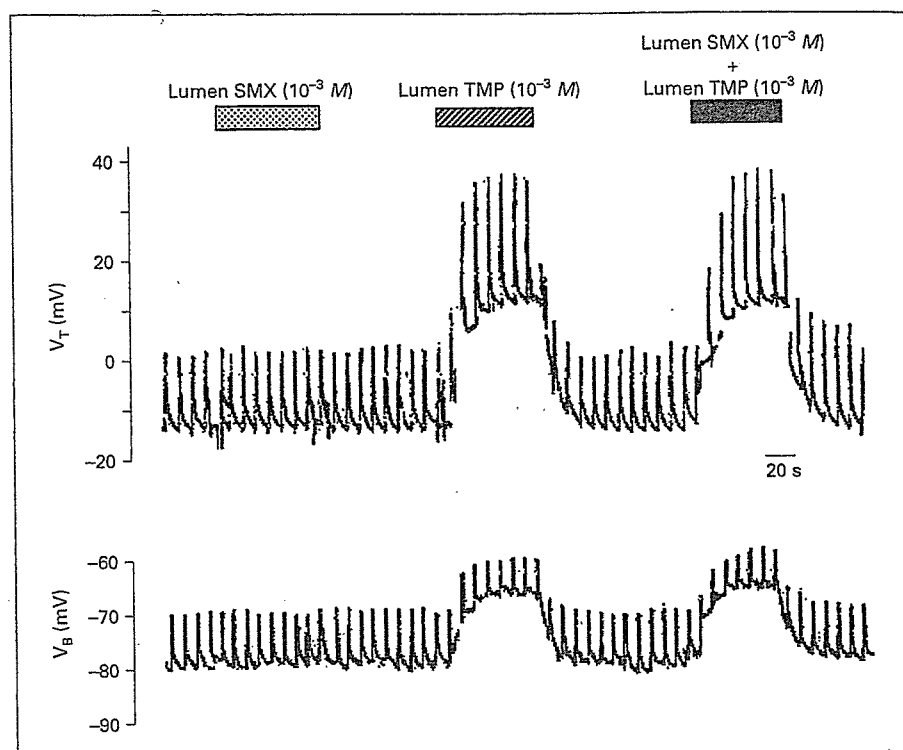


**Fig. 3.** Typical tracings showing effects of a separate or simultaneous addition of SMX and TMP at  $10^{-3} M$  to the lumen on  $V_T$  and  $V_B$  in the CCD. Voltage spikes are due to 50 nA constant-current pulses at 10-second intervals.

**Table 2.** Effects of SMX and TMP in the lumen on barrier voltages and resistances in the CCD

	Control	SMX ( $10^{-3} M$ )	Control	TMP ( $10^{-3} M$ )	Control	TMP ( $10^{-3} M$ ) + SMX ( $10^{-3} M$ )
$V_T$ , mV	$-10.5 \pm 1.0$	$-10.3 \pm 0.9$	$-10.4 \pm 0.8$	$18.0 \pm 5.5^+$	$-10.1 \pm 0.9$	$18.3 \pm 5.7^+$
$V_B$ , mV	$-79.4 \pm 3.4$	$-78.7 \pm 3.4$	$-80.8 \pm 3.2$	$-58.7 \pm 3.4^*$	$-80.7 \pm 3.4$	$-58.3 \pm 4.5^+$
$V_A$ , mV	$68.9 \pm 1.7$	$68.4 \pm 2.9$	$70.4 \pm 2.8$	$76.7 \pm 2.9^{++}$	$70.6 \pm 3.0$	$76.7 \pm 3.4^{++}$
$R_T$ , $\Omega \text{cm}^2$	$114.3 \pm 2.0$	$114.1 \pm 2.3$	$112.6 \pm 2.0$	$144.9 \pm 4.1^+$	$113.6 \pm 1.6$	$147.0 \pm 4.1^{++}$
$fR_A$	$0.41 \pm 0.04$	$0.40 \pm 0.04$	$0.40 \pm 0.04$	$0.48 \pm 0.04^{++}$	$0.40 \pm 0.04$	$0.48 \pm 0.04^{++}$

Data are mean  $\pm$  SE of 7 tubules. \*  $p < 0.01$ , +  $p < 0.005$ , ++  $p < 0.001$  compared with preceding period.

$-10.9 \pm 1.9$  to  $9.3 \pm 2.7$  mV ( $p < 0.001$ ) and from  $-81.0 \pm 1.3$  to  $-67.0 \pm 2.9$  mV ( $p < 0.005$ ), respectively, resulting in a significant hyperpolarization of  $V_A$  from  $70.1 \pm 2.1$  to  $76.3 \pm 2.2$  mV ( $p < 0.001$ ). At this time, the  $R_T$  and  $fR_A$  significantly increased from  $119.1 \pm 4.8$  to  $151.0 \pm 6.6 \Omega \text{cm}^2$  ( $p < 0.001$ ) and from  $0.45 \pm 0.09$  to  $0.53 \pm 0.09$  ( $p < 0.001$ ), respectively. When TMP was washed out from the luminal perfusate, the TMP-induced electrical changes were immediately eliminated. Figure 2 summarizes the concentration-response relationships for luminal addition of TMP on increases in  $V_A$ ,  $R_T$ , and  $fR_A$  ( $\Delta V_A$ ,  $\Delta R_T$ , and  $\Delta fR_A$ , respectively). The

$\Delta V_A$ ,  $\Delta R_T$ , and  $\Delta fR_A$  were greater with greater concentrations of TMP.

We next examined whether SMX acts directly on the apical membrane of the CD cell. For this purpose, we added SMX at  $10^{-3} M$  to the luminal perfusate, and then measured barrier voltages and resistances in the CCD. As shown in figure 3 and table 2, SMX at  $10^{-3} M$  in the lumen had no effect on barrier voltages or resistances. To exclude the possibility that there may be an interaction between TMP and SMX, we simultaneously added TMP and SMX at  $10^{-3} M$  in the lumen, and then observed the electrical parameters. The effects of simultaneous addi-



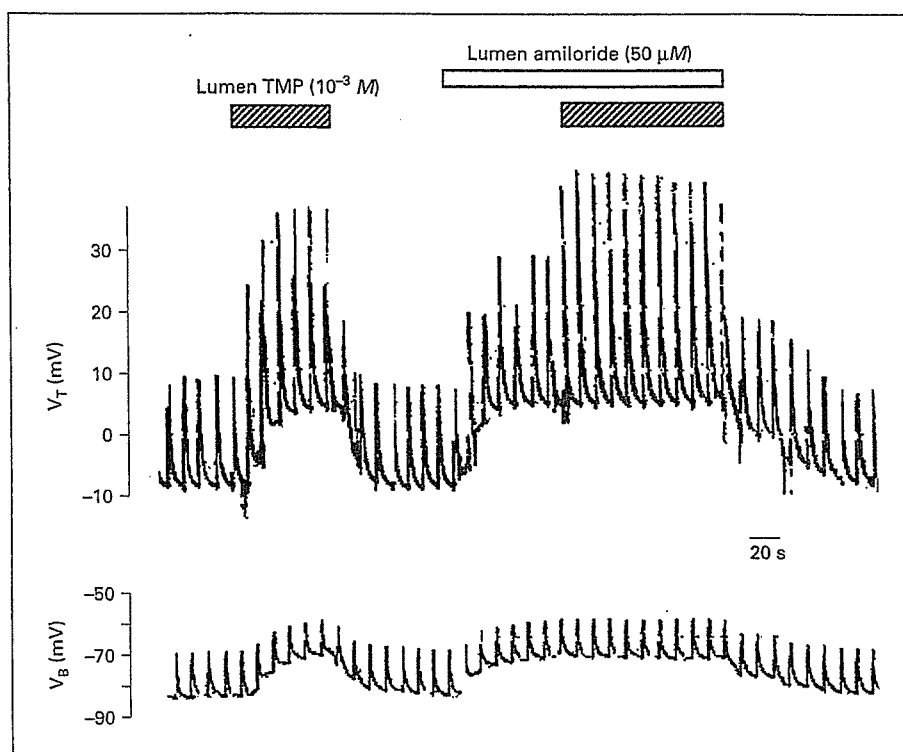


**Fig. 4.** Typical tracings showing effects of TMP ( $10^{-3} M$ ) in the lumen in the absence and presence of luminal amiloride ( $50 \mu M$ ) on  $V_T$  and  $V_B$  in the CCD. Voltage spikes are due to 50 nA constant-current pulses at 10-second intervals.

**Table 3.** Effects of TMP in the lumen in the absence and presence of luminal amiloride on barrier voltages and resistances in the CCD

	- Amiloride		+ Amiloride	
	- TMP	+ TMP	- TMP	+ TMP
$V_T$ , mV	$-5.4 \pm 0.7$	$5.2 \pm 0.6^*$	$6.8 \pm 0.6$	$6.9 \pm 0.8$
$V_B$ , mV	$-80.8 \pm 2.1$	$-74.5 \pm 2.0^*$	$-73.9 \pm 2.7$	$-73.6 \pm 2.8$
$V_A$ , mV	$75.3 \pm 2.2$	$81.3 \pm 2.5^*$	$80.8 \pm 2.5$	$80.5 \pm 2.6$
$R_T$ , $\Omega \text{cm}^2$	$112.3 \pm 4.4$	$146.2 \pm 6.9^*$	$148.9 \pm 8.6$	$148.4 \pm 9.4$
$fR_A$	$0.47 \pm 0.04$	$0.55 \pm 0.05^*$	$0.59 \pm 0.04$	$0.58 \pm 0.04$

Data are mean  $\pm$  SE of 9 tubules. The concentrations of TMP and amiloride were  $10^{-3} M$  and  $50 \mu M$ , respectively. The results as shown above were serial experiments in the absence and presence of luminal amiloride. \*  $p < 0.001$  compared with preceding period.

tion of TMP and SMX in the lumen on barrier voltages and resistances were extremely similar to those of TMP alone in the lumen, as shown in figure 3 and table 2.

The above-mentioned findings suggest to us the possibility that only TMP in the lumen may inhibit the apical membrane  $\text{Na}^+$  conductance in the CCD. To demon-

strate this possibility, we added a  $\text{Na}^+$  channel inhibitor amiloride ( $50 \mu M$ ) to the luminal perfusate, and then examined the effect of TMP ( $10^{-3} M$ ) in the continued presence of luminal amiloride on CD cell. Figure 4 shows a typical tracing showing the effect of TMP in the absence and presence of amiloride on  $V_T$  and  $V_B$ . Table 3 summarizes barrier voltages and resistances under the experimental conditions. When amiloride was added to the luminal perfusate, the lumen-negative  $V_T$  and  $V_B$  rapidly depolarized, resulting in a significant hyperpolarization of  $V_A$  by  $5.5 \pm 1.0$  mV ( $n = 9$ ). Luminal amiloride alone also significantly increased both  $R_T$  and  $fR_A$  by  $32.0 \pm 0.4 \Omega \text{cm}^2$  ( $n = 9$ ) and  $0.13 \pm 0.02$  ( $n = 9$ ), respectively. These results confirm our previous observations [12, 13, 15]. When TMP was added to the lumen in the continued presence of luminal amiloride,  $V_T$ ,  $V_B$ ,  $V_A$ ,  $R_T$ , or  $fR_A$  was no longer changed. These findings are compatible with the notion that TMP in the lumen actually inhibits amiloride-sensitive macroscopic  $\text{Na}^+$  conductance at the apical membrane of the CD cell.

To test the possibility that TMP in the lumen may directly inhibit apical membrane  $\text{K}^+$  conductance of the CD cell, we added  $\text{Ba}^{2+}$  ( $2 \text{ mM}$ ) to the lumen, and then observed the effect of TMP ( $10^{-3} M$ ) in the lumen in the continued presence of luminal  $\text{Ba}^{2+}$  on electrical proper-

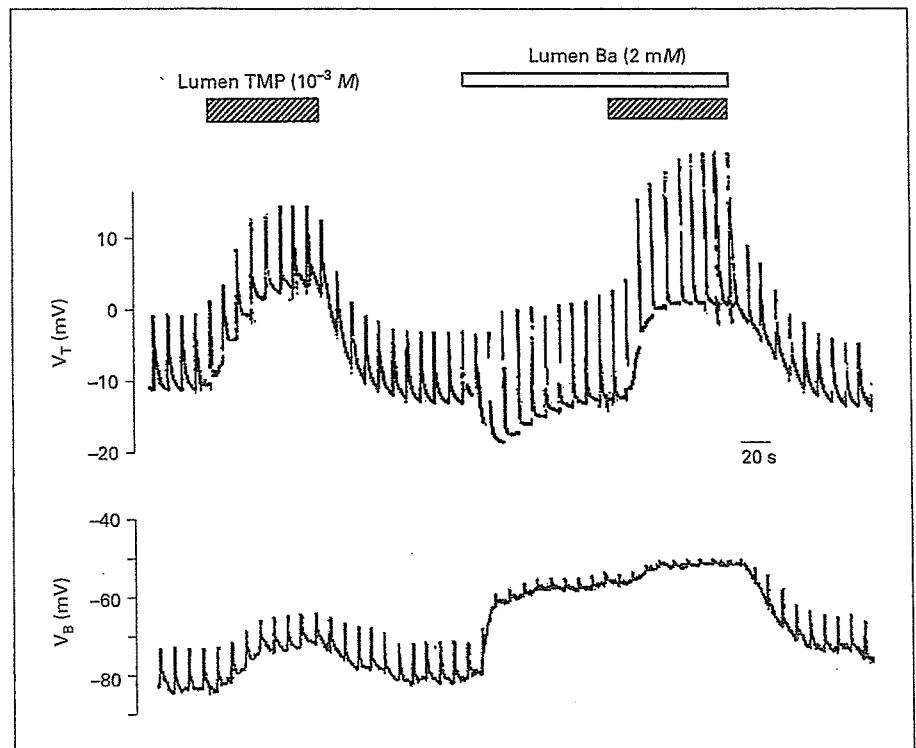


**Fig. 5.** Typical tracings showing effects of TMP ( $10^{-3} M$ ) in the lumen in the absence and presence of luminal  $Ba^{2+}$  ( $2 mM$ ) on  $V_T$  and  $V_B$  in the CCD. Voltage spikes are due to 50 nA constant-current pulses at 10-second intervals.

ties. Figure 5 shows a typical tracing showing the effect of TMP in the lumen in the absence and presence of luminal  $Ba^{2+}$  on  $V_T$  and  $V_B$ . Table 4 summarizes barrier voltages and resistances under the experimental conditions. When  $Ba^{2+}$  was added to the luminal perfusate, the lumen-negative  $V_T$  rapidly increased, and then slowly decreased to reach a new steady state level. The  $V_B$  rapidly depolarized within several seconds, and then slowly depolarized further to a new steady state level. Therefore,  $V_A$  rapidly depolarized during the first phase, and then slowly depolarized to a new steady state level. The biphasic effects of  $Ba^{2+}$  on  $V_T$ ,  $V_B$ , and  $V_A$  were similar to those reported previously [13, 15]. The transient current induced by luminal addition of  $Ba^{2+}$  is due to blocking the  $K^+$  current directed from cell to lumen. The  $V_T$  becomes more negative and the  $V_A$  becomes depolarized at first, because, after blocking the opposing  $K^+$  current, the net current is now only composed of the  $Na^+$  reabsorptive current. The circular  $Na^+$  current flow produced at the apical membrane causes the  $V_B$  to depolarize. In the second phase, the  $Na^+$  current relaxed probably due to several factors, i.e. first, a decrease in the driving force for  $Na^+$  entry, since  $V_A$  is depolarized by  $\sim 40$  mV; second, changes in intracellular ion content; and, finally, cell volume changes, because  $K^+$  exit is eliminated by  $Ba^{2+}$  [15].

**Table 4.** Effects of TMP in the lumen in the absence and presence of luminal  $Ba^{2+}$  on barrier voltages and resistances in the CCD

	- $Ba^{2+}$		+ $Ba^{2+}$	
	- TMP	+ TMP	- TMP	+ TMP
$V_T$ , mV	$-8.9 \pm 1.3$	$7.3 \pm 2.1^{**}$	$-9.5 \pm 1.4$	$4.1 \pm 2.0^{**}$
$V_B$ , mV	$-83.0 \pm 2.0$	$-73.4 \pm 3.1^*$	$-45.2 \pm 3.5$	$-39.7 \pm 4.1^*$
$V_A$ , mV	$73.2 \pm 1.7$	$80.2 \pm 2.2^{**}$	$35.3 \pm 3.3$	$42.9 \pm 3.4^{**}$
$R_T$ , $\Omega cm^2$	$115.0 \pm 3.6$	$151.6 \pm 4.2^{**}$	$216.8 \pm 10.2$	$252.6 \pm 10.7^{**}$
f $R_A$	$0.47 \pm 0.04$	$0.54 \pm 0.03^{**}$	$0.85 \pm 0.01$	$0.92 \pm 0.01^{**}$

Data are mean  $\pm$  SE of 11 tubules. The concentrations of TMP and  $Ba^{2+}$  were  $10^{-3} M$  and  $2 mM$ , respectively. The results as shown above were serial experiments in the absence and presence of luminal  $Ba^{2+}$ . \*  $p < 0.005$ , \*\*  $p < 0.001$  compared with preceding period.

Thus, both  $V_T$  and  $V_B$  slowly depolarize to a new steady state. Following addition of  $Ba^{2+}$  in the lumen,  $R_T$  increased by  $101.6 \pm 14.0 \Omega cm^2$  ( $n = 11$ ) and f $R_A$  increased by  $0.38 \pm 0.03$  ( $n = 11$ ). These findings also confirm our previous observations [13, 15]. When TMP was added to the luminal perfusate in the continued presence of luminal  $Ba^{2+}$ , both  $V_T$  and  $V_B$  further depolarized, resulting

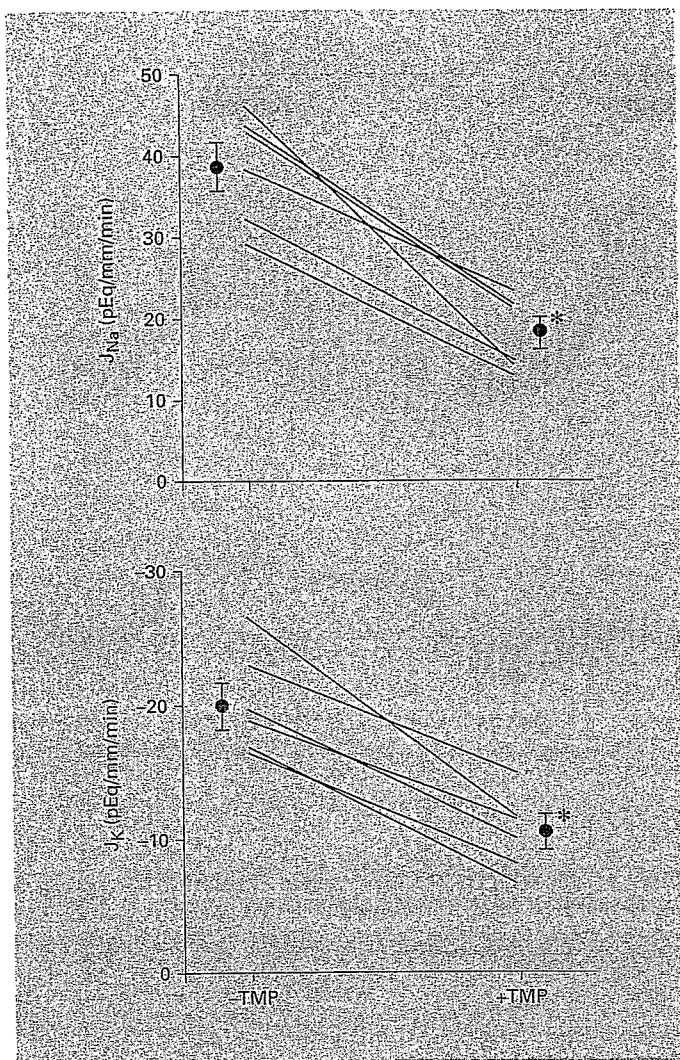


**Fig. 6.** Effects of TMP ( $10^{-3} M$ ) in the lumen on net  $\text{Na}^+$  and  $\text{K}^+$  fluxes in the same CCD segments. Asterisk indicates that the difference is significant (\* $p < 0.001$ ).

in a significant hyperpolarization of  $V_A$ . Under the experimental conditions, both  $R_T$  and  $fR_A$  further significantly increased. The increases in  $V_A$  or  $fR_A$  in the presence of  $\text{Ba}^{2+}$  and TMP ( $7.6 \pm 1.1$  mV or  $0.07 \pm 0.007$ , respectively) were not significantly different from those in the presence of TMP alone ( $7.0 \pm 0.8$  mV or  $0.07 \pm 0.009$ , respectively). Therefore, we concluded that TMP in the lumen did not inhibit apical membrane  $\text{K}^+$  conductance of the CD cell at all.

We next examined whether the luminal addition of TMP actually influences net transepithelial transports of  $\text{Na}^+$  and  $\text{K}^+$  in the CCD perfused in vitro. The results are shown in figure 6.  $J_{\text{Na}}$  and  $-J_{\text{K}}$  ( $n = 6$ ,  $18.1 \pm 2.1$  and  $10.5$

$\pm 1.3$  pEq/mm/min, respectively) in the presence of luminal TMP at  $10^{-3} M$  significantly decreased by 53.1 and 48.0% compared with those in its absence ( $n = 6$ ,  $38.6 \pm 3.0$  and  $20.2 \pm 1.7$  pEq/mm/min, respectively).

#### *Effect of TMP and SMX in the Bath on Electrical Properties of the CD Cell*

We finally examined whether TMP and/or SMX acts directly on the basolateral membrane of the CD cell. For this purpose, we individually added TMP and SMX at  $10^{-3} M$  to the bathing solution, and then observed the electrical parameters. As shown in figure 7 and table 5, TMP in the bath slightly but significantly depolarized  $V_T$  and  $V_B$  from  $-9.8 \pm 1.1$  to  $-8.4 \pm 0.9$  mV ( $p < 0.001$ ) and from  $-78.5 \pm 3.1$  to  $-77.0 \pm 3.3$  mV ( $p < 0.01$ ), respectively, without significant changes in  $R_T$  or  $fR_A$ , whereas SMX in the bath had no effect on barrier voltage or resistances. TMP at  $10^{-4}$  or  $10^{-5} M$  in the bath had no effect on barrier voltages or resistances (data not shown).

#### **Discussion**

In A6 cells, the apical addition of TMP has been reported to inhibit both amiloride-sensitive short circuit current [1] and  $\text{Na}^+$  channel activity [10]. The present study used microelectrode technique and flux measurements to examine the effects of TMP and SMX on electrical properties of the apical and basolateral membranes in the rabbit CCD perfused in vitro. We demonstrated that TMP, but not SMX, mainly acts on the apical membrane of the rabbit CCD and inhibits macroscopic  $\text{Na}^+$  conductance.

Urinary  $\text{K}^+$  excretion is largely the result of its secretion in CD cells [reviewed in 9, 18]. This is a two-step process that involves active uptake of  $\text{K}^+$  from blood to cell via the basolateral membrane  $\text{Na}^+$ - $\text{K}^+$  pump and passive diffusion from cell to lumen through a large apical membrane  $\text{K}^+$  conductance. Apical  $\text{Na}^+$  conductance is also involved in  $\text{K}^+$  secretion because it not only supplies most of  $\text{Na}^+$  for the basolateral  $\text{Na}^+$ - $\text{K}^+$  pump but it also depolarizes the apical membrane and thus facilitates  $\text{K}^+$  egress into the lumen.  $\text{K}^+$  secretion is regulated in CD cells by the supply of  $\text{Na}^+$ , the intake of  $\text{K}^+$ , by hormones such as mineralocorticoids and vasopressin, and by changes in blood pH and by many diuretics, including amiloride [9, 18].

In the current study, we found that TMP in the lumen hyperpolarized the apical membrane of the CD cell in

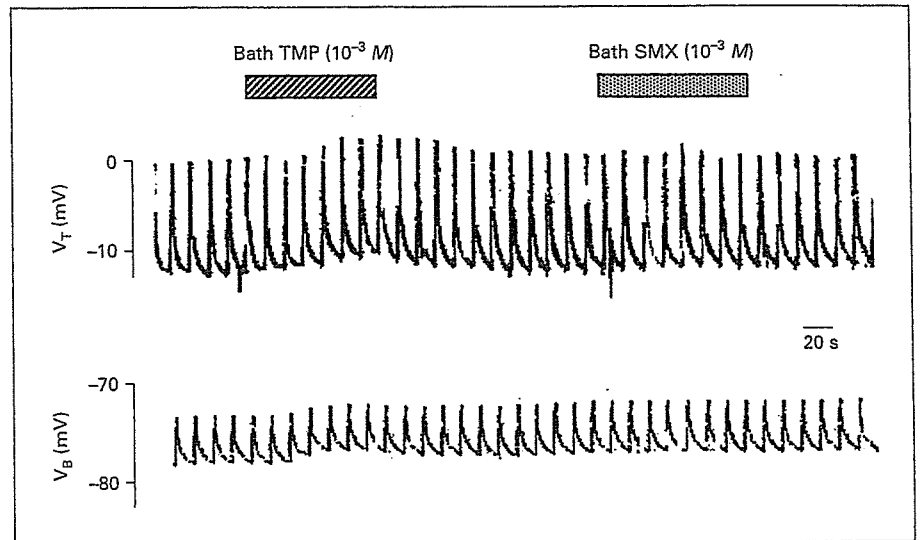


**Fig. 7.** Typical tracings showing effects of TMP and SMX at  $10^{-3} M$  in the bath on  $V_T$  and  $V_B$  in the CCD. Voltage spikes are due to 50 nA constant-current pulses at 10-second intervals.

**Table 5.** Effects of TMP and SMX at  $10^{-3} M$  in the bath on barrier voltages and resistances in the CCD

	Control	TMP ( $10^{-3} M$ )	Control	SMX ( $10^{-3} M$ )
$V_T$ , mV	$-9.8 \pm 1.1$	$-8.4 \pm 0.9^{**}$	$-9.7 \pm 1.1$	$-9.3 \pm 1.0$
$V_B$ , mV	$-78.5 \pm 3.1$	$-77.0 \pm 3.3^*$	$-78.4 \pm 2.8$	$-78.5 \pm 2.8$
$V_A$ , mV	$68.7 \pm 2.5$	$68.6 \pm 2.8$	$68.7 \pm 2.2$	$69.2 \pm 2.3$
$R_T$ , $\Omega\text{cm}^2$	$116.5 \pm 2.8$	$117.4 \pm 3.7$	$114.9 \pm 3.1$	$114.1 \pm 3.2$
$fR_A$	$0.47 \pm 0.04$	$0.47 \pm 0.04$	$0.47 \pm 0.05$	$0.46 \pm 0.04$

Data are mean  $\pm$  SE of 9 tubules. \*  $p < 0.01$ , \*\*  $p < 0.001$  compared with preceding period.

parallel with increases in  $R_T$  and  $fR_A$  in a concentration-dependent manner. The TMP-induced electrical changes were completely inhibited by luminal amiloride but not by luminal  $\text{Ba}^{2+}$ . TMP in the lumen also decreased both net  $\text{Na}^+$  reabsorption and  $\text{K}^+$  secretion in the CCD. These findings are consistent with the notion that TMP indeed acts on the apical membrane of the CD cell to inhibit the amiloride-sensitive macroscopic  $\text{Na}^+$  conductance in the rabbit CCD. Therefore, like amiloride, TMP in the lumen causes hyperpolarization of the apical membrane, reduces the net driving force for diffusion of  $\text{K}^+$  from cell to lumen, and thereby leads to an inhibition of  $\text{K}^+$  secretion.

In contrast to the action of TMP on the apical membrane, TMP at  $10^{-3} M$  in the bath caused a slight but significant depolarization of  $V_T$  and  $V_B$  without changes in  $R_T$  or  $fR_A$ . The findings suggest that TMP may act on the basolateral membrane of the CD cell and inhibit an elec-

trogenic  $\text{Na}^+$  transport system, possibly the  $\text{Na}^+-\text{K}^+$  pump activity. This is supported by the report of Eiam-Ong et al. [11], in which, when CCD segments isolated from normal rat kidneys were incubated with  $10^{-4} M$  TMP for 90 min, their  $\text{Na}^+-\text{K}^+-\text{ATPase}$  activities decreased by 30%, although the inhibitory effect of TMP at  $10^{-4} M$  on  $\text{Na}^+-\text{K}^+-\text{ATPase}$  activity in the rat CCD was much greater than that of TMP at  $10^{-3} M$  on basolateral  $\text{Na}^+-\text{K}^+$  pump activity in the rabbit CCD (fig. 7; table 5).

SMX at  $10^{-3} M$  in the lumen or bath had no effects on barrier voltages or resistances. Therefore, SMX in the lumen or bath had no effect on CD cell at all. Similarly, no effect of either apical or basolateral addition of SMX on amiloride-sensitive short circuit current [1] or highly selective  $\text{Na}^+$  channel activity [10] has been reported in A6 cell monolayers. Furthermore, there was no interaction between TMP and SMX in the lumen (fig. 3; table 2).